

**KfK 3575**  
**März 1984**

**Study of the Adsorption of  
Methyl Iodide and  
Molecular Iodine on  
Clean Uranium and  
Uranium Dioxide Surfaces  
by Means of X-Ray  
Photoelectron (XPS)  
and Auger Electron  
Spectroscopy (AES)**

**J. G. Dillard, H. Moers, H. Klewe-Nebenius, G. Kirch,  
G. Pfennig, H. J. Ache  
Institut für Radiochemie**

**Kernforschungszentrum Karlsruhe**



Kernforschungszentrum Karlsruhe  
- Institut für Radiochemie -

KfK 3575

Study of the Adsorption of Methyl Iodide and Molecular Iodine on  
Clean Uranium and Uranium Dioxide Surfaces by Means of  
X-Ray Photoelectron (XPS) and Auger Electron Spectroscopy (AES)

J.G. Dillard\*, H. Moers, H. Klewe-Nebenius, G. Kirch,  
G. Pfennig and H.J. Ache

Kernforschungszentrum Karlsruhe GmbH, Karlsruhe

---

\* Department of Chemistry, Virginia Polytechnic Institute and State  
University, Blacksburg, VA 24061, USA

Als Manuskript vervielfältigt  
Für diesen Bericht behalten wir uns alle Rechte vor

Kernforschungszentrum Karlsruhe GmbH  
ISSN 0303-4003

## ABSTRACT

The adsorption of methyl iodide as well as of molecular iodine on uranium metal and on uranium dioxide has been studied at 25 °C. Surfaces of the substrates were cleaned and characterized before and after exposure using X-ray photoelectron (XPS) and X-ray and electron induced Auger electron (AES) spectroscopy. Exposures amounted up to 1500 L CH<sub>3</sub>I on uranium metal, 1000 L CH<sub>3</sub>I on UO<sub>2</sub>, 100 L I<sub>2</sub> on uranium metal, and 75 L I<sub>2</sub> on UO<sub>2</sub> (1 L = 1 Langmuir = 10<sup>-6</sup> torr · sec). From the measured binding energies, Auger parameters, and intensity ratios for substrate and adsorbate constituents we deduced that for both CH<sub>3</sub>I and I<sub>2</sub> on uranium metal a uranium iodide, UI<sub>3</sub>, is formed. The adsorption of CH<sub>3</sub>I on U-metal is in addition accompanied by the formation of a carbide-type carbon, UC. Thus, in both cases a dissociative (adsorption/reaction) process is observed.

For adsorption of CH<sub>3</sub>I on UO<sub>2</sub> the experimental findings indicate a dissociative process, too, though the species formed could not be identified. In contrast, I<sub>2</sub> adsorption on UO<sub>2</sub> appears to have non-dissociative character.

Saturation coverages for CH<sub>3</sub>I were found to be ≈ 2 L on U-metal and ≈ 5 L on UO<sub>2</sub>, for I<sub>2</sub> ≈ 40 L on U-metal and 10-15 L on UO<sub>2</sub>.

Variations in the iodine Auger kinetic energy and in the Auger parameter are interpreted in light of extraatomic relaxation processes.

Untersuchung der Adsorption von Methyljodid und molekularem Iod an reinen Uran- und Urandioxid-Oberflächen mit Hilfe von Auger- und Röntgen-Photoelektronen-Spektroskopie

### ZUSAMMENFASSUNG

Die Adsorption von Methyljodid und molekularem Iod an Uranmetall und Urandioxid wurde bei 25 °C untersucht. U- und UO<sub>2</sub>-Oberflächen wurden gereinigt und vor und nach der Beladung mittels XPS und AES Spektroskopie charakterisiert. Die maximale Beladung betrug 1500 L CH<sub>3</sub>I auf Uranmetall, 1000 L CH<sub>3</sub>I auf UO<sub>2</sub>, 100 L I<sub>2</sub> auf U-Metall und 75 L I<sub>2</sub> auf UO<sub>2</sub> (1 L = 1 Langmuir = 10<sup>-6</sup> torr · sec). Aus den gemessenen Bindungsenergien, Augerparametern und Intensitätsverhältnissen für die Komponenten von Substrat und Adsorbat konnten wir schließen, daß bei der Adsorption von CH<sub>3</sub>I und I<sub>2</sub> auf U-Metall Urantrijodid entsteht. Bei der Adsorption von CH<sub>3</sub>I auf U-Metall wird außerdem Urancarbid - UC - gebildet. Folglich ist der Adsorptionsprozeß in beiden Fällen dissoziativ.

Bei der Adsorption von CH<sub>3</sub>I an UO<sub>2</sub> deuten die experimentellen Ergebnisse ebenfalls auf einen dissoziativen Prozeß hin. Eine Identifizierung der entstehenden Spezies war jedoch nicht möglich. Im Gegensatz hierzu scheint aber die Adsorption von molekularem Iod an UO<sub>2</sub> nicht dissoziativ zu sein.

Sättigung für die CH<sub>3</sub>I Adsorption wurde für U-Metall bei ≈ 2 L und für UO<sub>2</sub> bei ≈ 5 L erreicht, für die I<sub>2</sub>-Adsorption an U-Metall bei ≈ 40 L und an UO<sub>2</sub> bei 10-15 L.

Änderungen der kinetischen Energie der Auger Elektronen und in den Augerparametern werden auf der Basis von extra-atomaren Relaxationsprozessen diskutiert.

## Contents

	page
1. Introduction	1
2. Experimental Section	3
3. Results and Discussion	8
3.1 Characterization of Substrates: Uranium and Uranium Dioxide	8
3.2 Adsorption of Methyl Iodide on Uranium	14
3.2.1 Interpretation of XPS Spectra	16
3.2.2 Investigation of the Adsorbate Properties	20
3.2.3 Formation of a Uranium Triiodide Sublayer	25
3.2.4 Kinetics	26
3.3 Adsorption of CH <sub>3</sub> I on UO <sub>2</sub>	32
3.4 Adsorption of Molecular Iodine on Uranium Metal	36
3.4.1 Interpretation of XPS Binding Energies and AES Kinetic Energies	43
3.4.2 UI <sub>3</sub> Surface Layer Thickness	49
3.4.3 Kinetics	50
3.5 Adsorption of Molecular Iodine on Uranium Dioxide	53
3.5.1 Interpretation of XPS Binding Energies	53
3.5.2 Thermal Desorption	56
3.5.3 Kinetics	57
4. Summary	57
References	62

## 1. INTRODUCTION

Knowledge regarding the interaction of uranium metal and uranium oxide surfaces with gaseous molecules is important in many areas of actinide chemistry. Investigations of surface processes may aid in understanding the chemical, physical, and magnetic properties of uranium materials (1-5), in describing the chemical processes associated with oxidation and corrosion of uranium (6-10), and in discovering the reactions of gaseous radionuclides following fission. From these, radioiodine and its reactions deserve special attention due to its special biological influence (11-13). Interest in the surface characterization of uranium and uranium oxides is adequately demonstrated by publications reporting the XPS spectra of uranium metal and of uranium oxides (3-6,10,14-17). Auger studies of uranium metal, of uranium oxides, and of uranium following the reaction with molecular oxygen have been published (1,2,18,19). The emphasis in the previous studies has been to determine electron binding energies, to establish the nature and energy of shake-up satellite peaks, and to measure and assign the Auger transitions.

The interaction of dioxygen with clean uranium produces a  $\text{UO}_2$  phase when surfaces are free of carbon contamination (1,7). Under appropriate conditions a  $\text{UO}$  phase can be prepared by heating an  $\text{O}_2$  saturated uranium dioxide phase to  $700\text{ }^\circ\text{C}$  in vacuum and then cooling the sample to  $25\text{ }^\circ\text{C}$  (1). The reaction product following adsorption of dioxygen on a carbon contaminated surface is a  $\text{UO}_x\text{C}_y$  phase (10,8) which is difficult to characterize chemically.

In a study of the adsorption of water on uranium (7), XPS binding energy results were presented to support a dissociative process. The authors detected three  $\text{O } 1s$  photopeaks. The photopeak at high binding energy was attributed to water condensed on the surface, the middle peak to an  $\text{OH}$  complex with uranium. The third peak at lowest binding energy was assigned to oxygen, bond to uranium, although its binding energy was not equal to the  $\text{O } 1s$  binding energy after the reaction of dioxygen with uranium. It was suggested that the binding energy was shifted due to the presence of the  $\text{OH}$ -uranium complex. The reaction of dioxygen with uranium metal occurred more rapidly than the reaction of water with uranium under similar experimental conditions.

In the reaction of carbon and/or hydrocarbons with uranium, carbides are formed (20). The conditions for the formation of uranium iodides have been documented and the physical properties of uranium halides have been discussed (21-23).

Castleman et al. (11) have examined the chemical processes that take place for iodine produced via nuclear fission and released into steam and into steam plus added gases. In the release from uranium metal into steam, iodide is the primary product, whereas the iodine released from uranium dioxide occurs principally as  $I_2$ . Iodide is produced when iodine is released from  $UO_2$  into a gaseous environment composed of steam and hydrogen. Methyl iodide was also detected in this study and was believed to result from the reaction of iodine with carbon containing impurities in the system.

In a related study (13) the reactivity of propane with iodine produced from  $U_3O_8$  by fission and released in atmospheres of oxygen and of helium was investigated. In the temperature range 300-480 °C  $UI_n$  (n not defined) in a helium atmosphere was more reactive against propane than  $I_2$  generated in an oxygen atmosphere. Above 480 °C the reactivity of the iodine and  $UI_n$  species was similar.

In several of the previous studies (36,40,41,55-59) of diatomic halogen adsorption on metals it was of interest to discover periodic trends exhibited by halogens in adsorption kinetics and adatom substrate interactions (55,57,58) and to probe the variety of complex structures that are produced (36,40,41,56,59). Adsorption of iodine on uranium and on uranium dioxide is of fundamental and practical interest; however, many of the properties of these systems are unexplored.

From a practical point of view knowledge regarding the fate of iodine produced in nuclear reactors and adsorbed on aerosols is of particular interest with regard to health hazards (12,60,61), and studies of the reactions of iodine and iodine-containing molecules are important for an understanding of corrosion reactions involving reactor components (61,62).

The present work combines results from the investigation of adsorption and reaction processes of methyl iodide and molecular iodine on uranium metal and uranium dioxide. The principal goals have been to characterize well prepared clean substrate surfaces under ultra high vacuum conditions via X-ray photoelectron (XPS) and Auger electron (AES) spectroscopy and - after exposure to iodine and iodide - to obtain information on dissociative or non-dissociative nature of the adsorption process as well as on the chemical characteristics of the systems. Furthermore, the applicability of several kinetic models for description of the adsorption process is considered.

## 2. EXPERIMENTAL SECTION

The adsorption and surface characterization experiments were carried out using a Vacuum Generators ESCALAB-5 instrument. The instrument contains an analysis chamber, wherein XPS and AES spectra are measured, and a preparation chamber where interaction of gases with samples is carried out. Each chamber is pumped by a liquid nitrogen trapped turbomolecular pump, and pressures are measured using Bayard-Alpert ionization gauges. The analysis chamber is also pumped by a titanium sublimation pump. The base pressure in each chamber is  $5.0 \times 10^{-11}$  mbar ( $3.8 \times 10^{-11}$  torr). The X-ray gun is differentially pumped using an 8 l/sec Varian ion pump. Gases are introduced into the preparation chamber through a Vacuum Generators precision leak valve model MD-7 (all metal bellows-type valve) from a stainless steel gas reservoir system. The gas reservoir system is pumped using a molecular sieve trap in combination with an 8 l/sec Varian ion pump.

The instrument is interfaced to a Digital PDP 11/03-L computer and can be operated using the Vacuum Generators 4025 Data System software. The software package includes also programs for curve resolution (deconvolution), XPS inelastic background subtraction, spectral subtraction, depth and time profile studies, curve smoothing, differentiation, integration, and plotting. For these studies the instrument was operated using the computer mode to facilitate data acquisition, interpretation, and presentation.

The XPS data were acquired using Mg  $K_{\alpha}$  (1253.6 eV) or Al  $K_{\alpha}$  (1486.6 eV) radiation. Two X-ray anodes were used to permit the identification of photopeaks resulting from X-ray induced Auger transitions. XPS spectra were measured at take-off angles,  $\phi$ , equal  $10^{\circ}$  and  $80^{\circ}$  where  $\phi$  is the angle between the normal to the sample surface and a line along the direction to the analyzer entrance. Spectra were obtained at 100 watts for measurements with the Mg anode and at 240 watts when using the Al anode. Electron kinetic energies were measured using a hemispherical analyzer operated at a pass energy of 20 eV. The Au  $4f_{7/2}$  full-width-at-half-maximum (FWHM) at 20 eV analyzer pass energy was 1.2 eV. Binding energies are referenced to the Fermi level of the substrates. The Fermi level was established by setting the maximum for the U 5f photopeak at 0.5 eV for uranium metal (3-5) and at 1.6 eV for uranium dioxide (3,7,9,17). XPS peak intensities were calculated from integrated photopeak intensities and included the intensity of shake-up satellite peaks. The integrated photopeak intensities were evaluated from the raw data after the following treatment: The

raw data were smoothed using a 15 point routine; the X-ray satellite contribution was subtracted using intensities and positions given by Carlson (24) and confirmed by measuring the X-ray satellite intensity for clean gold. Inelastic electron background was removed using a function suggested by Shirley et al. (25). The atomic ratios were evaluated from the integrated photopeak intensities using photoionization cross sections published by Scofield (26) and an empirically determined instrumental sensitivity factor. The relative sensitivity factors for carbon and iodine were determined by measuring the XPS and AES spectra for a thick layer of  $\text{CH}_3\text{I}$  condensed at  $-196^\circ\text{C}$  on gold and on an oxidized aluminum surface. In these sensitivity determinations XPS spectra were measured for different time intervals at 50 and 100 watts (Mg anode). During the measurements no alteration in the relative peak areas (XPS) was noted.

Electron induced Auger electron spectra were determined using 1.5 keV and 5.0 keV electrons. Sample currents were of the order of 0.4 to 1.0  $\mu\text{A}$  during the AES measurements. AES spectra were determined routinely using a retard ratio of 2. However, in an attempt to record iodine  $\text{M}_4\text{N}_{4,5}\text{N}_{4,5}$  spectra following the adsorption of  $\text{I}_2$  on  $\text{UO}_2$  a retard ratio of 4 was used. Auger peak intensities were evaluated by measuring the peak-to-peak heights in the derivative spectra for the following transitions where the approximate energies (eV) are given in parentheses: uranium OPV (73), NOV (284); iodine  $\text{M}_5\text{N}_{4,5}\text{N}_{4,5}$  (507),  $\text{M}_4\text{N}_{4,5}\text{N}_{4,5}$  (518.5); oxygen KLL (510); carbon KLL (274). The carbon KLL Auger peak intensity was determined using 1.5 keV electrons so that contributions to the signal from the uranium NOV transition (284 eV) were smaller than when using 5 keV electrons. Peak intensities for iodine Auger transitions induced by 5 keV electrons were used since the signal to noise ratio was better at this energy. Absolute energies for the Auger transitions were determined by measuring the peak maxima for the X-ray induced Auger transitions and then correcting the electron induced spectra accordingly (35a).

The experimental conditions for exposure and XPS and AES measurements did not allow an exact reproducibility of the sample geometry since e.g.

- exposure and measurements were performed in different chambers,
- after long sputtering a contamination was deposited on the X-ray gun window causing a reduced X-ray flux,
- optimum sample positions for XPS and AES are different, and
- adsorbate layers were not proved to be fully homogeneous.

Consequently intensity ratios are presented rather than absolute intensity results using experimentally measured correction factors for conversion of intensity data to atomic ratios. The reproducibility of the intensity results for repetitive exposures is  $\pm 5\%$  on uranium and  $\pm 15\%$  on uranium dioxide. The inaccuracy of the adsorption isotherm data may be greater than  $\pm 10\%$  since the pressure was measured using an ionization gauge not calibrated for  $\text{CH}_3\text{I}$  or  $\text{I}_2$ . However, the measured pressure may be reasonable since two factors may be compensating: First, the sensitivity of the gauge for  $\text{CH}_3\text{I}$  and  $\text{I}_2$  is probably greater than the sensitivity for  $\text{N}_2$ . This fact would yield a pressure reading greater than the actual pressure in the preparation chamber during the exposure. However, this condition could be offset by a second fact: the ionization gauge is located near the liquid nitrogen trap and the turbopump at a distance of about 50 cm from the samples. Considering this second point the actual pressure at the sample could be higher than that measured. The apparatus is not equipped with a means for measuring the absolute quantity of  $\text{CH}_3\text{I}$  or  $\text{I}_2$  present during or after the exposure.

Polycrystalline uranium foil (0.1 mm) was obtained from Nuklear Chemie und Metallurgie, Frankfurt. From the foil circular disks (8.0 mm diameter) were cut, immersed in 6n  $\text{HNO}_3$  for 5 minutes, washed with distilled water and acetone, dried with a tissue, and affixed to a circular nickel probe (8.0 mm diameter) using silver paint as an adhesive. The uranium/Ag adhesive/Ni probe assembly was air dried for about 20 minutes using a red heat lamp and was inserted in the vacuum system. Uranium was cleaned in the analysis chamber using the following procedure which is similar to that described by Ellis (1). The probe was transferred to the analysis chamber which had been baked previously to attain a base pressure of  $5.0 \times 10^{-11}$  mbar. Uranium was heated to 600 °C\*) while etching with 5-6 keV  $\text{Ar}^+$  ions continuously for 24-36 hours. The metal was then repeatedly heated to 600 °C for 30 minutes, argon ion etched for 30 minutes at this temperature, annealed at 300-400 °C, and cooled to 25 °C. When AES spectra indicated that traces of carbon and oxygen had been removed, ( $< 0.1$  atomic %), the adsorption experiments were carried out using the following procedure. Uranium metal was transferred into the preparation chamber ( $p < 2.0 \times 10^{-10}$  mbar) and exposed to  $\text{CH}_3\text{I}$  or  $\text{I}_2$  at pressures in the range

---

\*) All temperatures quoted in this work refer to nominal values corresponding to the temperature control readings. The actual temperatures are expected to be about 15 % lower due to an unavoidable gradient between the thermocouple position and the sample surface.

$4 \times 10^{-9}$  to  $1 \times 10^{-7}$  mbar for the time necessary to obtain the desired exposure. The sample was then transferred back into the analysis chamber for XPS and AES measurements.

Following each exposure and the subsequent XPS/AES measurements the sample was cleaned as described above, checked for cleanliness by measuring the Auger spectrum, and used again. Thus, each data point in the adsorption curves corresponds to a measurement for  $\text{CH}_3\text{I}$  or  $\text{I}_2$  adsorbed on clean, annealed uranium. When clean uranium was transferred from the analysis chamber to the preparation chamber and held in the preparation chamber without exposure to  $\text{CH}_3\text{I}$  ( $\text{I}_2$ ) for a period of time equivalent to that used in the exposure process, subsequent XPS and AES spectra indicated that no carbon, oxygen or iodine signals were detected. Thus, the measured carbon and iodine signals can only arise as a result of adsorption and reaction processes and do not arise from sample contamination in the transfer process.

Uranium dioxide surfaces were prepared in two different ways, both exhibiting identical spectroscopic features. For the adsorption of  $\text{CH}_3\text{I}$  it was prepared from clean uranium metal exposed at 25 °C to 150 L of dioxygen, heated to 300-400 °C for 15 minutes, and cooled to 25 °C. This surface was treated with an additional 75 L  $\text{O}_2$ , and heated to 300-400 °C for 15 minutes, and cooled to 25 °C. The XPS and AES spectra of this material were equivalent to those reported by Ellis (1), Allen, et al. (6,14), and others (3,4,15-17). Because the  $\text{UO}_2$  surface is less reactive than a uranium surface (see Results and Discussion), the exposure experiments could be conducted by preparing a  $\text{UO}_2$  surface and then exposing this surface repeatedly to  $\text{CH}_3\text{I}$  to obtain the adsorption profile. Several different  $\text{UO}_2$  surfaces were prepared, characterized, and exposed to  $\text{CH}_3\text{I}$ . The quantity of  $\text{CH}_3\text{I}$  adsorbed did not vary outside the precision of reproducibility when comparing adsorption on different  $\text{UO}_2$  preparations.

For the adsorption of molecular iodine the uranium dioxide surface was prepared by thermal and  $\text{Ar}^+$  ion induced decomposition of  $\text{U}_3\text{O}_8$ . A pressed pellet of  $\text{U}_3\text{O}_8$  was heated at 600 °C for 12 hours and continuously ion etched with 5 keV  $\text{Ar}^+$  ions. Following annealing at 300 °C and cooling to 25 °C the XPS and AES spectral features were identical to those obtained for  $\text{UO}_2$  prepared by the reaction of  $\text{O}_2$  with uranium metal. Specifically the  $\text{UO}_2$  ( $\text{U}_3\text{O}_8 \rightarrow \text{UO}_2$ ) had a  $\text{U } 4f_{7/2}$  binding energy  $380.5 \pm 0.1$  eV, shake-up satellite peaks at 6.8 eV above each  $\text{U } 4f$  photopeak, and a  $\text{O } 2p/\text{U } 5f$  intensity ratio equal to 0.8. All of these parameters are in excellent agreement with those for previously prepared

stoichiometric  $\text{UO}_2$  ( $\text{U} + \text{O}_2 \rightarrow \text{UO}_2$ ) (6,15). Following  $\text{I}_2$  adsorption and XPS/AES surface measurements, a clean  $\text{UO}_2$  surface was regenerated by heating the  $\text{UO}_2 : \text{I}_2$  sample to 600 °C for 30 minutes while etching the surface with 5 keV  $\text{Ar}^+$  ions. The sample was then annealed at 600 °C for further 15-30 minutes and cooled to 25 °C over a 15 minutes period.

Methyl iodide, purchased from C. Roth GmbH & Co KG, Karlsruhe, had a stated purity of 99.5 %, and was used without additional purification. Gas chromatographic analysis indicated that no other organoiodides were present ( $< 0.1$  %) which could interfere in this study. Methyl iodide was stored in the dark in a refrigerator until transfer to a sample cylinder. The liquid was degassed by repetitive freeze-thaw cycles on a vacuum line ( $p = 1 \times 10^{-6}$  torr) that contained greaseless stopcocks and connectors. The degassed material was transferred to a 10  $\text{cm}^3$  stainless steel cylinder that had been degassed and dried by heating (400 °C) on the vacuum line. The sample vessel was further "conditioned" by condensing  $\text{CH}_3\text{I}$  in the cylinder and then evacuating the cylinder. This procedure was repeated several times, before  $\text{CH}_3\text{I}$  was condensed into the cylinder for these studies.

Iodine was purchased from Merck, Darmstadt, as doubly sublimed reagent grade and was used without additional purification. The iodine was placed in a cleaned and preconditioned stainless steel cylinder. The preconditioning was accomplished by introducing iodine into the cylinder, pumping away the  $\text{I}_2$ , and then reintroducing  $\text{I}_2$ .

The gas doser system and the preparation chamber of the XPS/AES instrument were conditioned by introducing  $\text{CH}_3\text{I}$  or  $\text{I}_2$  into these chambers and pumping the gases away several times. Only after this pretreatment of the gas inlet system and the preparation chamber reproducible results could be obtained. Unfortunately, in case of iodine the pressure could not be maintained constant throughout each exposure, so pressures in the range  $4 \times 10^{-9}$  to  $2 \times 10^{-8}$  mbar were recorded as a function of time and these incremental exposures summed to give the total exposure.

Oxygen (99.995 % purity) was obtained from Messer-Griesheim GmbH, Düsseldorf. It was transferred to a clean and dry stainless steel cylinder which was then attached to the doser vacuum system.

### 3. RESULTS AND DISCUSSION

#### 3.1 Characterization of Substrates: Uranium and Uranium Dioxide

The preparation of clean, well characterized surfaces was an important first step in this study. The Auger spectrum for uranium measured using 5 keV electrons (Fig. 1) is like that reported by Ellis (1) and Bastasz and Felter (19). An examination of the peak intensities in the expanded energy regions for carbon and oxygen illustrates that the surface concentration of these elements is less than 0.1 atomic %. The XPS spectrum for clean uranium (Fig. 2) is typical of spectra obtained following the preparation of clean uranium as described in the experimental procedures. The binding energies for the uranium 4f photopeaks summarized in Table 1 are in agreement with the values reported by previous investigators (5,6,16,27). The full-width-at-half-maximum (FWHM) for the U 4f levels is 1.7 eV whereas the values shown earlier were 1.4 (7), 1.8 (5) and 2.7 eV (6). It is not clear whether these differences are attributable to differences in instrumental parameters used in measuring the spectra or arise from partial contamination of the metal surface by reactions with background gases (6). The uranium valence band spectrum (Fig. 2) is similar to that reported by other investigators (3,5,7), but does not contain the shoulder at about 2 eV which is present in the spectrum published by Veal and Lam (4). The authors indicate that some surface contamination was unavoidable in their study. Thus, we attribute our AES and XPS spectra to clean uranium metal and have used the spectral features of both surface characterization methods to assure the preparation of clean uranium before the exposure of uranium to methyl iodide or iodine.

The AES and XPS spectra for uranium dioxide are illustrated in Figs. 3 and 4, respectively. The AES spectra agree with those published by others in terms of peak energy positions and peak shapes (1,2). They do not exhibit the features noted by Ellis (8) for a  $\text{UO}_2$  surface contaminated with oxycarbide layers.

Many authors have discussed the XPS spectra of the core and valence band levels for  $\text{UO}_2$  and for non-stoichiometric uranium dioxides, i.e.  $\text{UO}_{2+x}$  (3-6,9,10,14-17). From these earlier studies, it appears that a stoichiometric  $\text{UO}_2$  surface can be characterized using U 4f binding energies, the energy positions of the U 4f shake-up satellite features (14,15), and the relative peak intensities of the O 2p and U 5f photopeaks at energies within 10 eV of the Fermi level (3-5,9,10,16,17). A comparative evaluation of these spectral features is much more definitive in identifying a stoichiometric  $\text{UO}_2$  surface than the consideration of either U 4f

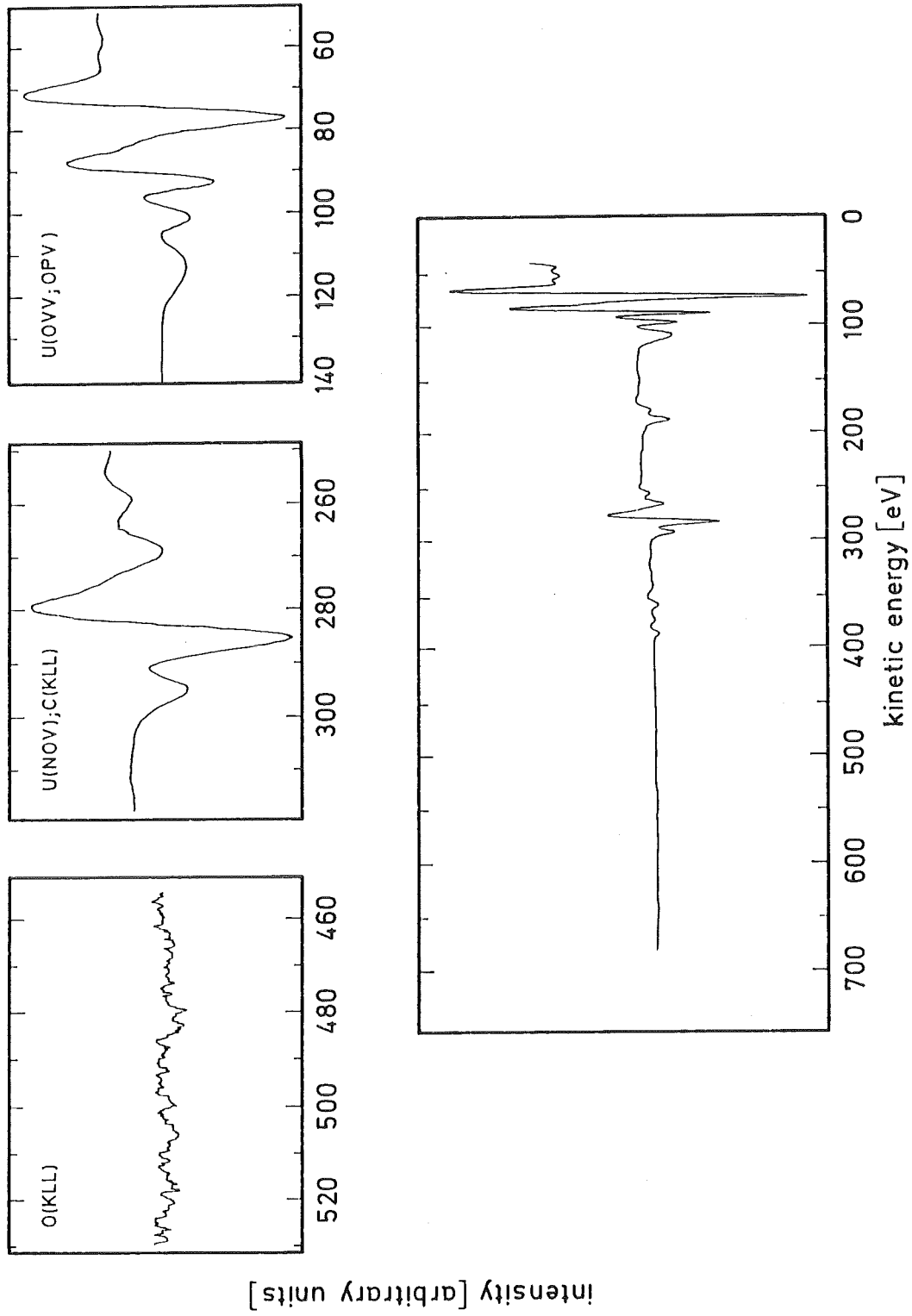


Fig. 1: Auger electron spectra using 5 kV electrons for clean uranium

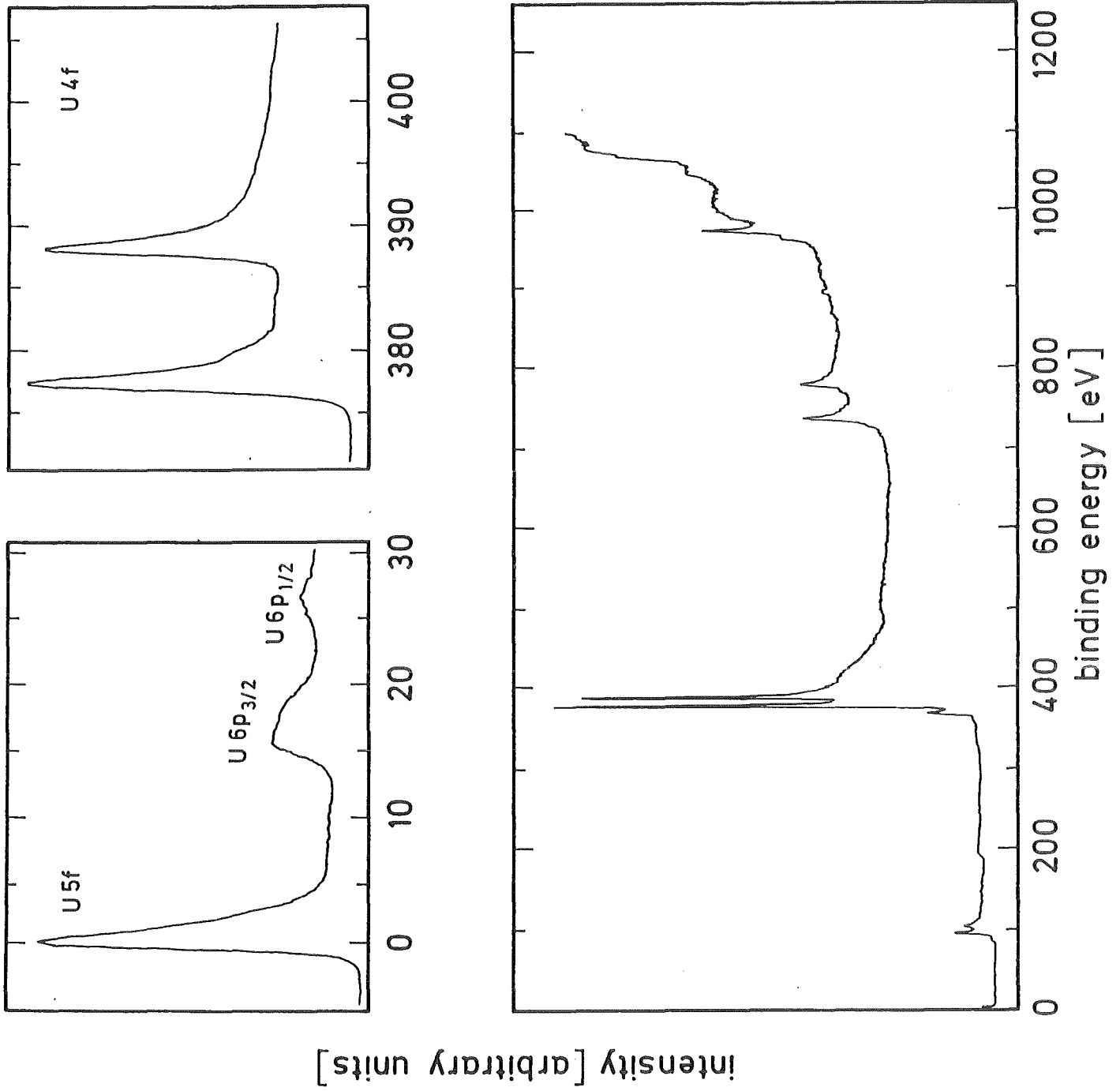


Fig. 2: X-ray photoelectron spectra (Mq anode) for clean uranium

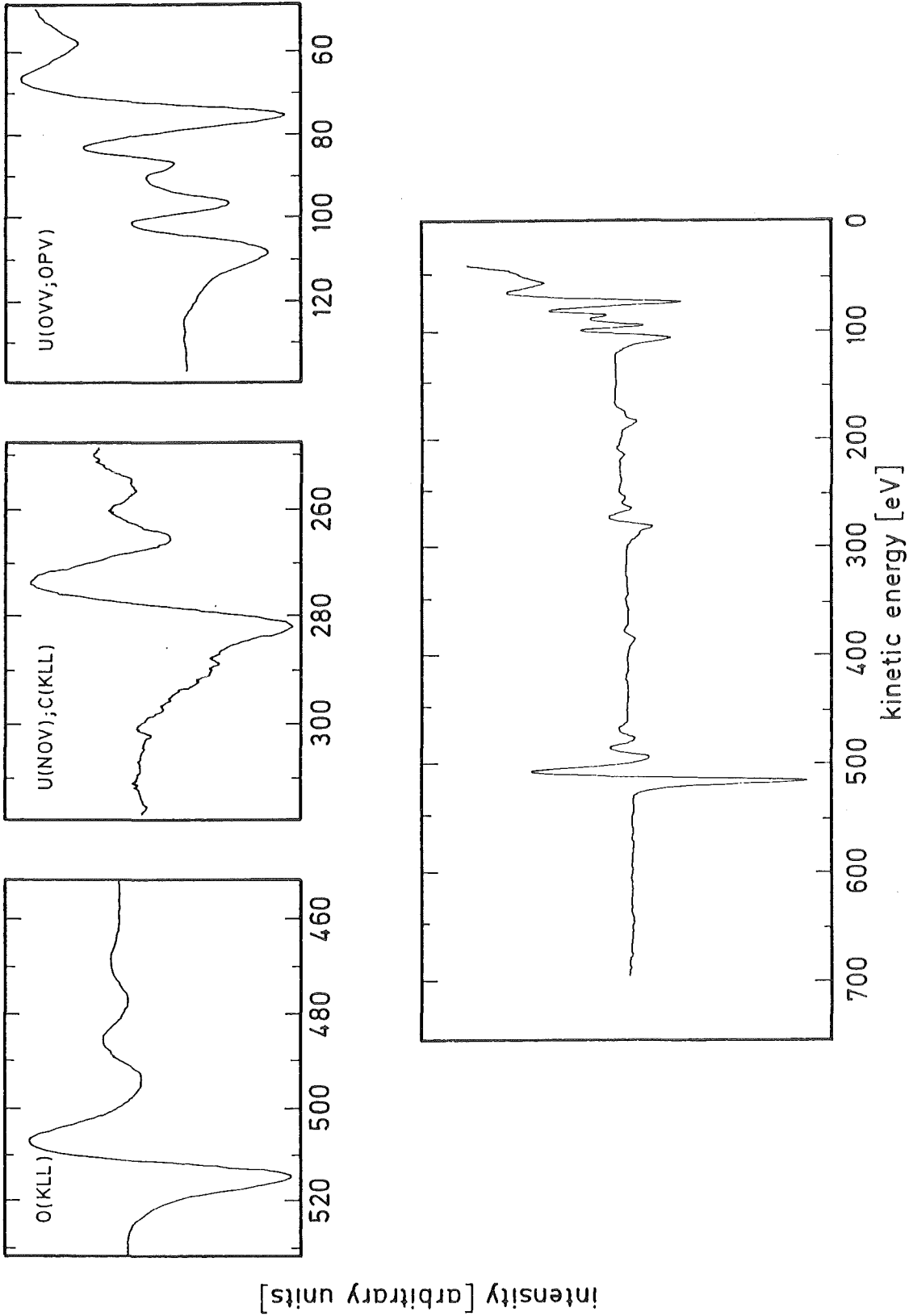


Fig. 3: Auger electron spectra using 5 kV electrons for clean uranium dioxide

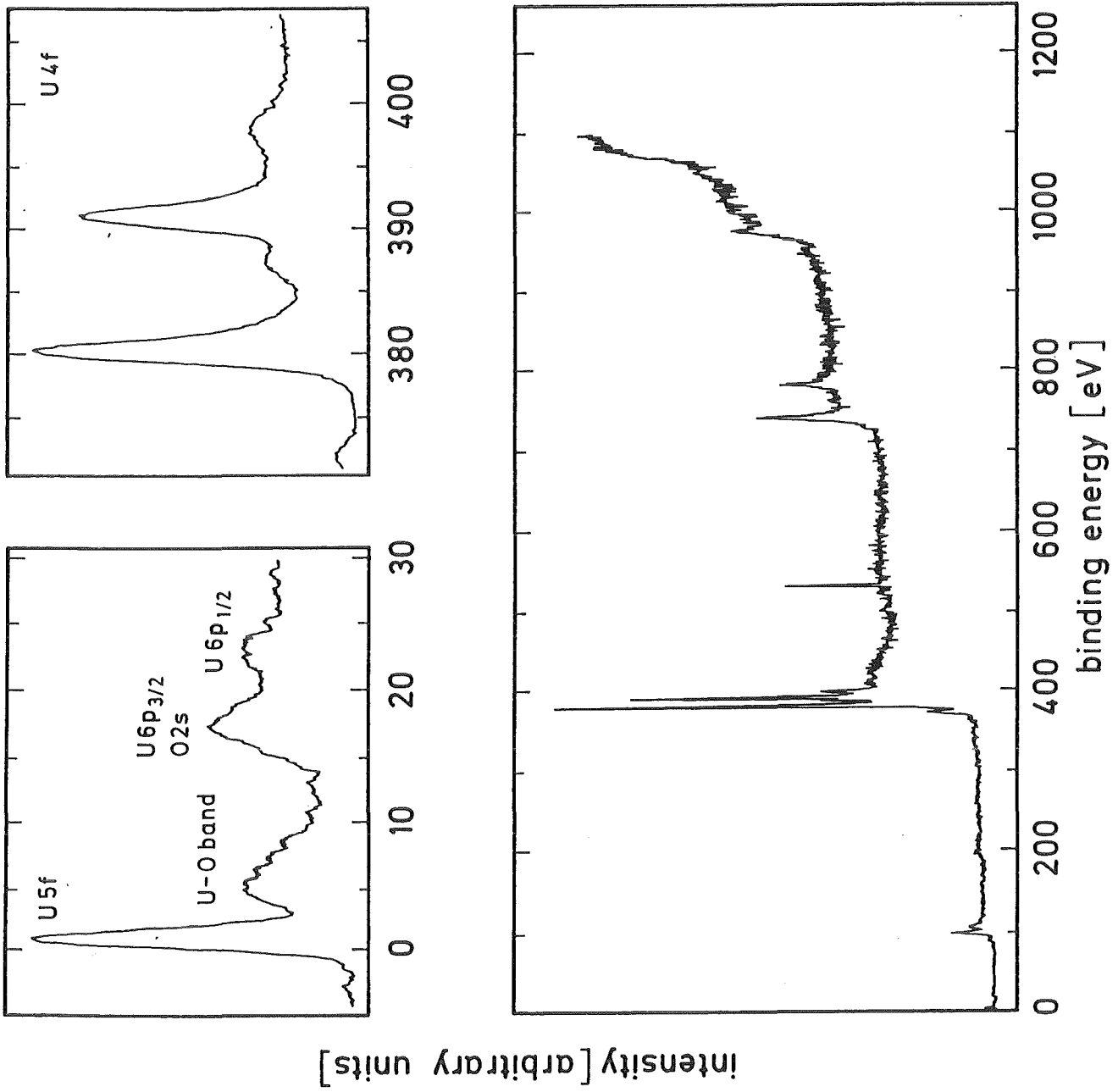


Fig. 4: X-ray photoelectron spectra (Mg anode) for clean uranium dioxide

Table 1: XPS Binding Energy Results for Uranium Containing Substrates

Level	Binding Energy eV	FWHM eV	Reference
<u>Uranium metal</u>			
U 4f <sub>7/2</sub>	377.4 ± 0.1	1.7	(+)
	377.4 ± 0.2	1.8	(5,27)
	377.1 ± 0.3	2.7	(6)
	377.2	n.g.	(16)
	378.0	1.4	(7)
U 4f <sub>5/2</sub>	388.3 ± 0.1	1.8	(+)
	388.2 ± 0.2	n.g.	(5,27)
	387.8 ± 0.3	n.g.	(6)
<u>Uranium dioxide</u>			
U 4f <sub>7/2</sub>	380.5 ± 0.1	2.1	(+)
	380.8 ± 0.2	1.8	(15)
	380.9 ± 0.2	2.0	(5,27)
	380.3	2.6	(14)
	380.1 ± 0.3	2.1	(6)
	380.5	n.g.	(16)
satellite	387.4 ± 0.1	n.g.	(+)
	387.1	n.g.	(14)
	387.0	n.g.	(6)
	387.8	n.g.	(15)
U 4f <sub>5/2</sub>	391.4 ± 0.1	2.2	(+)
	391.2	2.6	(14)
	391.7 ± 0.2	2.1	(15)
	391.7 ± 0.2	n.g.	(5,27)
satellite	398.2 ± 0.1	n.g.	(+)
	398.0	n.g.	(14)
	398.5	n.g.	(15)

n.g.: line width not given

+ : values from the present work

binding energies or U 4f satellite features or the relative intensity of the O 2p and U 5f energy levels alone (9,10,14,15,17). The uranium 4f binding energy (380.5 eV) measured in this study is in good agreement with values reported in the literature and summarized in Table 1. The U 4f XPS spectra for stoichiometric UO<sub>2</sub> exhibit shake-up satellite peaks which are reported at 6.7 eV (9), 6.8 eV (14), or 6.9 eV (average, ref. 15) above the main U 4f photopeaks. For non-stoichiometric UO<sub>2+x</sub>, two pairs of satellite peaks appear at 6.9 eV (14,15) and at 8.2 eV (14,15) above the main U 4f photopeaks. The U 4f spectra for UO<sub>2</sub> prepared for this study (Fig. 4) show shake-up satellite peaks at 6.9 eV (U 4f<sub>7/2</sub>) and at 6.8 eV (U 4f<sub>5/2</sub>) above the main U 4f peaks.

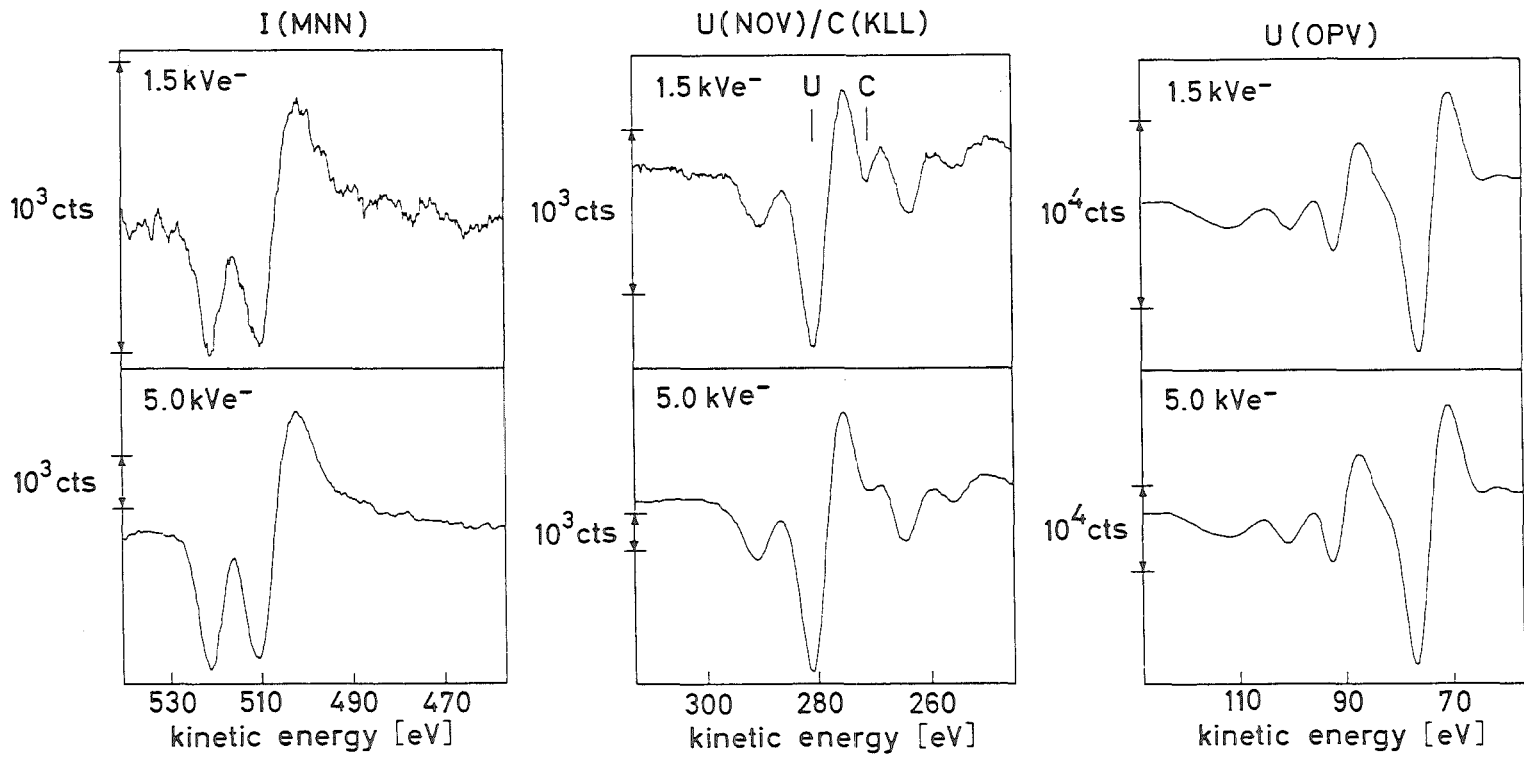
The valence band spectrum for UO<sub>2</sub>, also shown in Fig. 4, exhibits peaks attributable to U 5f, O 2p, and U 6p transitions. Beatham et al. (9) have recorded a valence band spectrum for stoichiometric UO<sub>2</sub> from which an O 2p/U 5f integrated peak intensity ratio equal to 0.8 was calculated. It has been argued (9) that an intensity ratio greater than 0.8 (17) is indicative of the presence of non-stoichiometric oxide phases. Unfortunately, no core level U 4f spectra were presented by Evans (17) from which U 4f shake-up satellite features could be inspected to indicate the presence of UO<sub>2+n</sub> phases. In the present study, the preparations of UO<sub>2</sub> yielded an O 2p/U 5f ratio of 0.7 to 0.8. This ratio is in good agreement with the ratio calculated for stoichiometric UO<sub>2</sub> (9).

It should also be mentioned that long term (15 hours) XPS scans in the C 1s region for the UO<sub>2</sub> surfaces prepared here revealed no signal attributable to surface carbon contamination which could arise in the preparation of UO<sub>2</sub> or from background gases in the spectrometer. From a consideration of binding energies, satellite structural features, and relative peak intensities in the valence band region, we conclude that the surfaces prepared for the adsorption studies are clean, stoichiometric UO<sub>2</sub> surfaces.

### 3.2 Adsorption of Methyl Iodide on Uranium

The adsorption of CH<sub>3</sub>I was studied for exposures up to 1500 L. Auger spectra recorded using 1.5 keV and 5.0 keV electrons for uranium metal exposed to 2 L CH<sub>3</sub>I are shown in Fig. 5. The energy regions of interest for iodine and for carbon illustrate the appearance of the spectra from which peak-to-peak intensity measurements were carried out. An XPS spectrum for the binding energy range 0-1100 eV (Mg K<sub>α</sub> radiation) and expanded spectra for the U 4f,

Fig. 5: Auger electron spectra using 1.5 and 5.0 kV electrons following the exposure of clean uranium to 2 L CH<sub>3</sub>I



I 3d, C 1s, and valence regions are given in Fig. 6 for an exposure of 150 L CH<sub>3</sub>I on uranium metal. The appearance of the U 4f XPS spectra in Fig. 2 and in Fig. 6 and the corresponding Auger U(OPV) spectra in Fig. 1 and Fig. 5, show no significant changes following the adsorption of CH<sub>3</sub>I. These spectra are representative of those that were recorded for all exposures up to saturation coverage. (The experimental fractional coverage  $\theta$  is equal to one at saturation).

### 3.2.1 Interpretation of XPS Spectra

Representative XPS binding energy and Auger parameter<sup>\*)</sup> results are summarized in Table 2 for uranium surfaces following exposure to CH<sub>3</sub>I. The Auger parameter results for methyl iodide condensed at -196 °C are also presented in Table 2. Because of difficulties in obtaining an accurate energy calibration following the condensation of CH<sub>3</sub>I, only binding energy differences are given. The  $\Delta BE(I 3d_{5/2} - C 1s)$  for condensed CH<sub>3</sub>I is in reasonable agreement with differences measured for the gas phase molecule (31) and suggests that there is no significant degradation of condensed CH<sub>3</sub>I during the XPS measurements.

Throughout the CH<sub>3</sub>I exposure range there is no measurable change in the binding energies for the adsorbate or substrate atom photopeaks. In addition, the FWHM for I 3d<sub>5/2</sub> (1.8 eV), for C 1s (1.5 eV), and for U 4f<sub>7/2</sub> (1.7 eV) did not vary by more than the precision of the measurements,  $\pm 0.1$  eV, for all exposures.

The binding energies for adsorbed carbon indicate that surface reactions have accompanied CH<sub>3</sub>I adsorption. The C 1s binding energy, 282.0 eV, does not change as a function of exposure, and the value is less than the 285 eV value normally associated with hydrocarbon-type carbon (24). In addition, the difference in the I 3d<sub>5/2</sub> and C 1s binding energies is greater than the corresponding difference for pure CH<sub>3</sub>I (31). If no chemical alteration occurred upon adsorption, it is expected that the difference in I 3d and C 1s binding energies would be unchanged. The C 1s binding energy is equal to the binding energy for carbon in stoichiometric uranium carbide (UC) which is somewhat greater than the values reported for transition metal carbides (32). However, the

---

\*) The Auger parameter  $\alpha$  is defined as the sum of photoelectron binding energy and Auger electron kinetic energy for selected transitions of the same element (29).

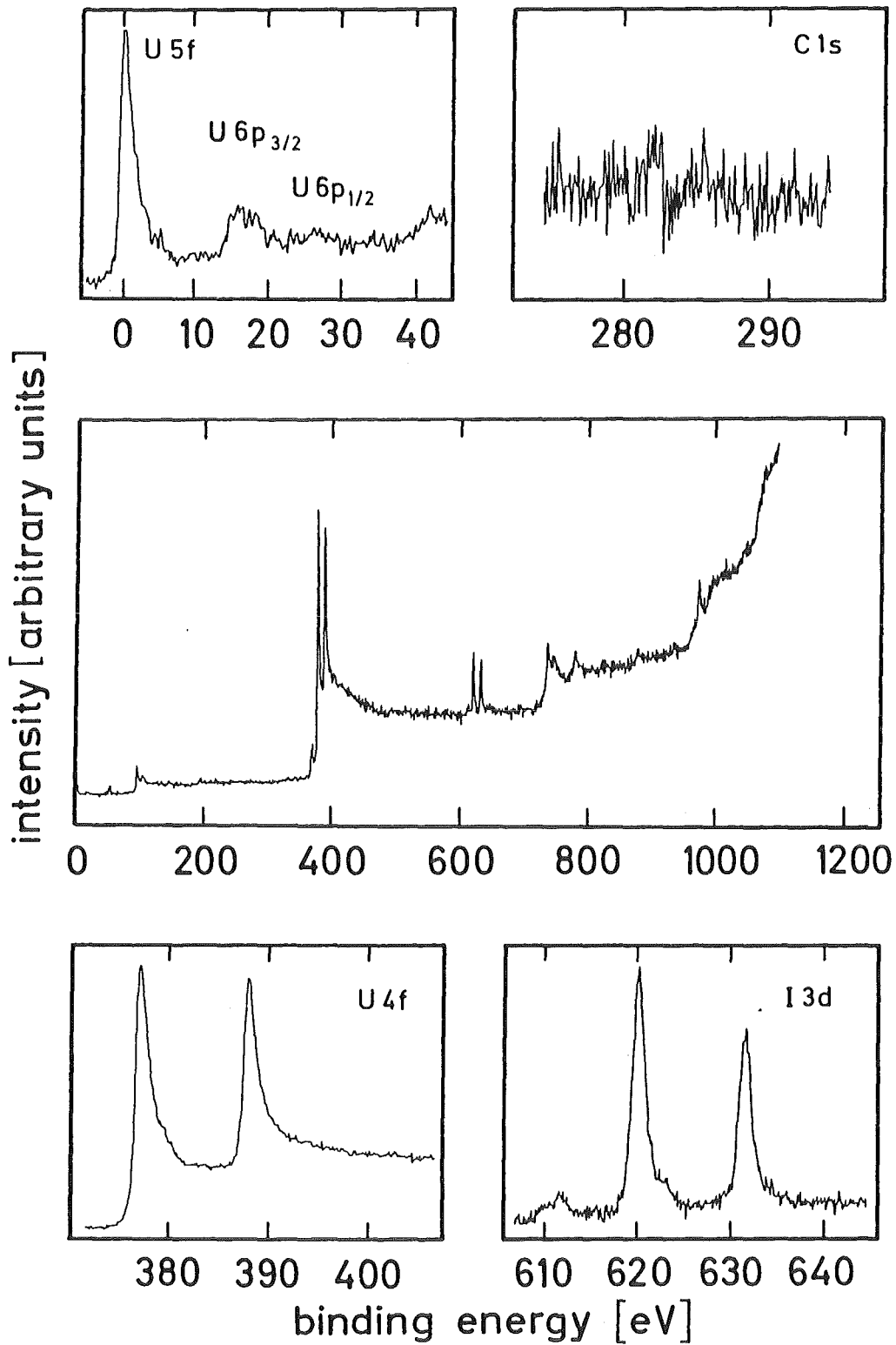


Fig. 6: X-ray photoelectron spectra (Mg anode) for uranium following exposure to 150 L CH<sub>3</sub>I

Table 2: XPS and AES Energies (eV) for CH<sub>3</sub>I Adsorption on U and UO<sub>2</sub>

CH <sub>3</sub> I Exposure (Langmuir)	U 4f <sub>7/2</sub> (±0.1)	I 3d <sub>5/2</sub> (±0.1)	C 1s (±0.1)	ΔE(I 3d <sub>5/2</sub> -C 1s)	I (M <sub>4</sub> NN) (±0.3)	Auger Parameter (α)
<u>Uranium metal</u>						
0	377.4	-	-	-	-	-
0.5	377.4	620.3	282.1	338.2	518.8	1139.1
1.0	377.4	620.3	282.0	338.3	518.8	1139.1
5.0	377.4	620.3	282.1	338.2	518.8	1139.1
10.0	377.4	620.2	282.1	338.1	518.8	1139.0
50.0	377.4	620.2	282.0	338.2	518.9	1139.1
1500.0	377.4	620.2	282.0	338.2	519.0	1139.2
<u>Uranium dioxide</u>						
0	380.5	-	-	-	-	-
1.0	380.5	620.3	-	-	-	-
2.0	380.5	620.3	-	-	-	-
5.0	380.4	620.4	-	-	-	-
10.0	380.5	620.4	-	-	-	-
50.0	380.4	620.4	285.4	335.0	-	-
1000.0	380.5	620.4	-	-	-	-
<u>Compound</u>	<u>Ref.</u>					
I <sub>2</sub> (s)	(38,39)	620.5				
I <sub>2</sub> (s)	(42)	619.9				
UI <sub>3</sub>	(+)	379.0	620.3		517.2	1137.5
UC	(+)	378.5	-	282.0		
CH <sub>3</sub> I(s)	(+)	-	-	-	335.3	-
CH <sub>3</sub> I(g)	(31)	-	626.66	291.43	335.23	
Ag/I <sub>2</sub> (ads)	(36)		619.3			
AgI(s)	(44)		619.4			
AgI(s)	(43)		618.2			

+ : values from the present work

good agreement of the C 1s binding energies for carbon following adsorption of CH<sub>3</sub>I and for carbon in UC indicates that a dissociative adsorption process occurs and that uranium carbide is a principal product. The formation of surface carbides in adsorption is not novel. Surface carbides are produced in the adsorption of hydrocarbons on tungsten (33) and on iron (34). It was suggested (34) that the carbide layer on iron inhibits further reaction of hydrocarbons with the surface and that poisoning of iron for catalytic hydrogenation of hydrocarbons is probably due to carbide formation.

The I 3d<sub>5/2</sub> binding energy is equal to the value determined for UI<sub>3</sub> in the present work. However, this close agreement does not prove that iodine is present as UI<sub>3</sub>, rather than other UI<sub>n</sub> (n = 1,2,4) species or atomic iodine. Thibaut et al. (37) found that the chlorine and bromine binding energy shifts for a series of U(III) and U(IV) halides and oxyhalides are less than 0.4 eV. The shifts are smaller for bromine compounds. Iodides were not studied. Thus large differences in the iodine binding energies would not be expected for UI<sub>3</sub> compared to UI<sub>4</sub>. However, Thibaut et al. (37) have noted that the electron binding energy shifts in uranium halides indicate a significant change from ionic to covalent bonding in proceeding from uranium fluorides to uranium bromides. Based on the former study (37) we predict that for a highly covalent uranium-iodine bond a small chemical shift in I 3d electron binding energy would be anticipated. The shift in the I 3d<sub>5/2</sub> photopeak compared to that in solid I<sub>2</sub> is -0.2 eV (38,39) or +0.4 eV (42). It could be argued that such a small difference in binding energy for adsorbed iodine (from CH<sub>3</sub>I) compared to molecular I<sub>2</sub> is within the experimental precision and thus would suggest the presence of molecular iodine. That molecular iodine is not present can be demonstrated from studies of XPS spectra following a series of thermal treatments of the sample after adsorption of CH<sub>3</sub>I. The discussion of the thermal studies is found later in this paper.

In a limited number of studies XPS was used to probe the chemical nature of adsorbed iodine species on metals (36,40,41). In the study of I<sub>2</sub> adsorption on Ag (36) iodine and silver electron binding energies and peak shapes plus additional spectral features were used to suggest the adsorption of iodine in a form unlike that found in AgI. It is clear from a comparison of the iodine 3d<sub>5/2</sub> binding energy results (Table 2) for solid iodine (38,39,42), for silver iodide (43,44), and for iodine (I<sub>2</sub>) adsorbed on silver (36) that the binding energies do not differ significantly and that taking alone the binding energies is not definitive in establishing the presence of atomic or ionic iodine. In the present study the binding energies for adsorbed iodine are equal to the value found in UI<sub>3</sub>. It is not

possible to predict whether the binding energy for atomic iodine adsorbed on uranium would be unequal to that for iodide in  $UI_3$ . Based on the binding energies alone we cannot state whether significant electron transfer has occurred from uranium to iodine upon adsorption of  $CH_3I$ . To inquire further into the nature of adsorbed iodine, the iodine  $M_4N_{4,5}N_{4,5}$  X-ray induced Auger transition was studied.

### 3.2.2 Investigation of the Adsorbate Properties

Wagner and coworkers (28-30) have used the Auger parameter for the identification of the chemical nature of surface species. Auger chemical shifts are usually greater than those for XPS binding energies because of the large screening effect in the doubly charged final ion. Detailed experimental and theoretical treatments of this phenomenon have been reported for metals and metal compounds (44,45,63). In these treatments the energy shifts are quantified by calculating atomic and extra-atomic relaxation energies. It has been shown (30,44,45,63) that the relative magnitude of the Auger parameter is related to the relaxation energy. We note that the kinetic energy for the I ( $M_4N_{4,5}N_{4,5}$ ) transition following  $CH_3I$  adsorption does not change in going from low to saturation coverage and thus the Auger parameter is unchanged.

However, the Auger parameter increases along the series:  $CH_3I$  condensed on Au or  $Al_2O_3$  <  $UI_3$  <  $CH_3I$  adsorbed on U. For  $CH_3I$  on Au or  $Al_2O_3$ , effects on the Auger parameter due to interaction of physisorbed  $CH_3I$  with the substrate (Au or  $Al_2O_3$ ) are negligible (46) since the measurements were made using multilayers of  $CH_3I$ . Further, we take the view that relaxation in condensed  $CH_3I$  could only be promoted by carbon or iodine atoms in neighboring molecules. Thus, the Auger parameter value for condensed  $CH_3I$  represents a reference point from which to gauge the magnitude of relaxation in the U- $CH_3I$  system. The shifts in the Auger parameter (relative to condensed  $CH_3I$ ) are 1.2 eV ( $UI_3$ ) and 2.9 eV ( $CH_3I/U$ ), respectively. In interpreting these results, we assume that adsorbed iodine (from  $CH_3I$ ) is present as iodide, an assumption which seems reasonable recognizing that adsorbed carbon (from  $CH_3I$ ) is converted to carbide and recalling the known chemistry of iodine and uranium (22). Based on the results for metals and metal compounds (28-30,44,45,63), we suggest that the Auger parameter shifts arise primarily from extra-atomic relaxation. Extra-atomic relaxation is presumed to be more important than atomic relaxation when making comparisons among different iodine species (28,42,45). Because the

Auger kinetic energy is not sensitive to coverage and because the iodine-iodine near neighbor distances must be large at low coverage (unless island formation occurs), near neighbor polarization screening by iodides is probably not significant in the extra-atomic relaxation process. An alternate source for polarization could be substrate uranium atoms near the adsorbed iodide. The uranium atoms contain unpaired 5f electrons at the metal valence band. Kowalczyk et al. (63) recognized that low binding energy metal valence electrons may be the principal electrons responsible for relaxation and noted a dramatic decrease in the extra-atomic relaxation effect for first row transition metals when proceeding from early period elements to copper and zinc. It was argued that such a decrease arises from reduced availability of d electrons due to filling of the d subshell which occurs at copper. In the case of uranium the low binding energy 5f orbitals are partially filled and could be involved in polarization screening of adsorbed iodine. The lower kinetic energy for the  $M_{4,5}N_{4,5}$  transition and the smaller Auger parameter for iodine in  $UI_3$  compared to adsorbed iodine (from  $CH_3I$ ) on uranium is no doubt related to a minimized screening effect that arises from the presence of oxidized uranium in  $UI_3$ .

Wertheim et al. (36) have reported for  $I_2$  adsorption on Ag that adatom core hole relaxation by substrate conduction electrons is the most significant extra-atomic relaxation process. The added relaxation process, core hole induced electron transfer to iodine from the substrate, is ruled out because low energy satellite features were not detected (36). In the present study we are not able to assess the relative probability of these two extra-atomic processes because the iodine photopeak intensity is too low. Additionally, the low binding energy spectral region is not a convenient region to study because X-ray satellite structure is subtracted in our treatment of the raw data and we cannot be completely sure that any remaining peak structure could be attributable to low energy satellite structure. In actual fact, after removal of the X-ray satellite structure we do not observe any residual structure that could be assigned to satellites, but we are not certain as to what the intensity of such peaks might be.

The  $I(M_{4,5}NN)$  energy position has not permitted an identification of adsorbed iodine as atomic iodine or ionic iodide, but has provided an interpretation of the Auger chemical shift based on relaxation effects. If we accept that iodine is present as iodide and likely as  $UI_3$ , then the Auger chemical shift that we measure for adsorbed iodide indicates that polarization effects related to relaxation phenomena in adsorption are significant when compared to corresponding changes among halides in simple metal salts (44).

Thibault et al. (37) commented that alterations in valence band spectra were not as prominent as those found for core levels. In our measurements we find that the valence band spectra for clean uranium and for uranium saturated with CH<sub>3</sub>I are identical. This is explained by the fact that the quantity of iodine and carbon on the surface is small.

An estimate of the surface concentration for carbon and iodine at saturation can be calculated from the expression published by Madey et al. (47) and modified by Roberts (48) to permit calculations using the cross section results of Scofield. The resulting expression is:

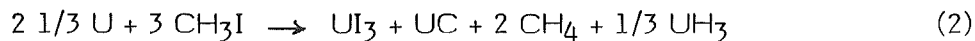
$$c = \frac{A}{S} \cdot \frac{\rho N \lambda \cos \phi}{M} \quad (1)$$

- where  $c$  = surface atom concentration: atoms/cm<sup>2</sup>  
 $A/S$  = adsorbate to substrate XPS intensity ratio, corrected for ionization cross sections (26) and instrumental sensitivity factors ( $A/S = 0.3$  for I 3d<sub>5/2</sub> to U 4f<sub>7/2</sub> and 0.09 for C 1s to U 4f<sub>7/2</sub>)  
 $\rho$  = substrate density (19.05 g/cm<sup>3</sup> for uranium)  
 $N$  = Avogadro's number  
 $\lambda$  = electron mean free path for the substrate (taken as 12 Å (24) for the U 4f<sub>7/2</sub> electrons at 876 eV kinetic energy)  
 $\phi$  = the electron take-off angle, relative to the surface normal (10° in these experiments)  
 $M$  = atomic/molecular weight of the substrate (238.07 g/mole for uranium)

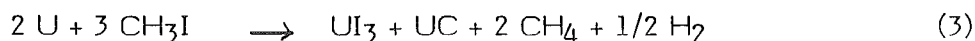
The iodine and carbon surface concentrations at saturation are calculated to be  $1.7 \times 10^{15}$  atoms/cm<sup>2</sup> and  $5.1 \times 10^{14}$  atoms/cm<sup>2</sup>, respectively. If we estimate the concentration of uranium atoms in the surface as  $\approx 1.3 \times 10^{15}$  atoms/cm<sup>2</sup> and make the assumption that one adsorbate atom per surface uranium atom represents monolayer coverage ( $\Gamma = 1.0$ ), it follows that the adsorption of CH<sub>3</sub>I yields  $\Gamma = 1.7$ . On the other hand, if it is assumed that adsorbed methyl iodide reacts with surface uranium to yield UI<sub>3</sub> and UC, the number of uranium surface atoms interacting with iodine becomes  $5.7 \times 10^{14}$  atoms/cm<sup>2</sup>, the total uranium surface atoms bound to adsorbate atoms is  $1.1 \times 10^{15}$ , and  $\Gamma = 0.83$ .

In experiments, where the adsorption and reaction of  $I_2$  with uranium was studied (see sect. 3.4 below), it was found that a surface concentration of  $\sim 3 \times 10^{15}$  iodine atoms/cm<sup>2</sup> was necessary to detect changes in the uranium XPS and Auger spectral features which could be related to oxidation of uranium. It is reasoned that, even if surface oxidation of uranium occurs upon adsorption of  $CH_3I$  to produce UC and  $UI_3$ , the surface concentration of oxidized uranium is too low to be detected.

The I/U and C/U atomic ratios at saturation are 0.3 and 0.09, respectively. The I/C ratio is very close to the ratio expected if the formation of surface  $UI_3$  and UC occurs in the ratio of 1:1. For this we must write the following equations for the surface reactions:



or



We are able only to speculate on the nature of products in addition to  $UI_3$  and UC. We formulate a uranium hydride as  $UH_3$  since this is the most stable form (21,22). The production of  $CH_4$  and  $UH_3$  or  $H_2$  is dictated by the stoichiometry of the adsorbate molecule. During these experiments no equipment for the detection of  $CH_4$  or  $H_2$  was available and the formation of surface  $UH_3$  could not be confirmed.

Uranium samples exposed to  $CH_3I$  were heated to selected temperatures for various time intervals and the XPS and/or AES spectra measured either at the temperature of the thermal treatment or at reduced temperatures, 25 °C or -196 °C. In all measurements the relative intensity ratios were not dependent on the temperature at which spectra were measured. The results of these measurements are presented in Fig. 7 where we show the variation in the I/U XPS or AES ratio as a function of the temperature for the thermal treatment. The results demonstrate that up to 600 °C (the maximum temperature attainable in our apparatus, but cf. footnote on p. 7) there is only a slight decrease in the I/U ratio. There was no change in the photoelectron or in the Auger spectral features. These findings, when combined with data on the physical properties of uranium iodides, limit the suggestions for possible surface uranium iodides. Using the vapor pressure equation for  $UI_4$  (22), the vapor pressure for  $UI_4$  at 600 °C is greater than 200 torr. Considering that the heat treatment at 600 °C lasted for

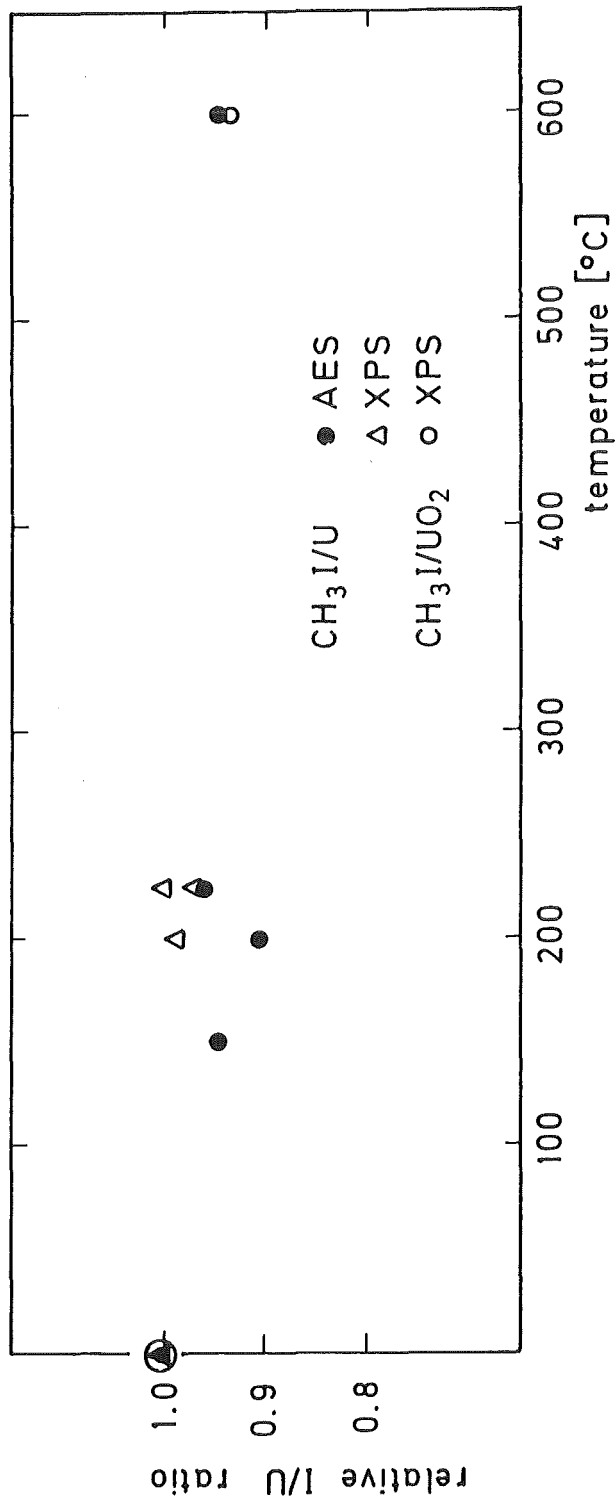


Fig. 7: I/U: XPS (atomic) and AES (intensity) ratios following exposure to CH<sub>3</sub>I and heating at various temperatures

15 hours, any  $UI_4$  present would be lost via vaporization. It is reasonable that the surface uranium iodide is not  $UI_4$ . In the adsorption of  $I_2$  on uranium,  $UI_3$  was identified (cf. sect. 3.4). For  $CH_3I$  adsorption  $UI_3$  is a likely surface species, but the presence of lower oxidation state uranium iodides  $UI_n$  ( $n = 1$  or  $2$ ) cannot be ruled out. The lower valent iodides would be expected to exhibit vapor pressure properties similar to those of  $UI_3$ . The formation of lower valent uranium iodides would be novel in that a common oxidation state for the actinide elements is +3 with the +2 state being more stable at the end of the period. Considering that the I/C atomic ratio is 3 following  $CH_3I$  adsorption and that the thermal properties of the uranium iodide surface are similar to those for  $UI_3$ , we conclude that lower valent uranium iodides are not produced in the adsorption of  $CH_3I$ , and that  $UI_3$  likely is the uranium surface iodide species.

The relative intensity for the C/U ratio did not change following the heat treatments. This finding seems reasonable since refractory uranium carbide (22) would not be expected to vaporize at the temperatures used in our experiments.

### 3.2.3 Formation of a Uranium Triiodide Sublayer

Dowben and Jones (49) have studied the adsorption of  $CBr_4$  and  $CCl_4$  on iron. The adsorption reaction was dissociative with the formation of a carbide sublayer over which a bromine adlayer was produced. Upon thermal treatment of iron following adsorption of  $CBr_4$  or  $CCl_4$ , the carbon concentration was reduced to zero before halogen desorption began. From this observation it was suggested that carbon was diffusing into the bulk. We find neither desorption nor apparent diffusion of the adsorbate atoms. It seems that stable uranium carbide and iodide are formed but that diffusion of the constituent atoms is slow. A possible reason for this result is that  $CH_3I$  exhibits a preferred orientation in its reaction with uranium such that the iodide or methyl portion of  $CH_3I$  adsorbs to produce a surface that is unreactive. We investigated the adsorption of  $CH_4$  on clean uranium to model the reactivity of the  $CH_3$ -group of  $CH_3I$  (50). The adsorption of methane on clean uranium at 25 °C and at 600 °C is not observed for  $CH_4$  exposures up to about 100 L. If we accept the modelling concept, the results suggest that the hydrocarbon portion of  $CH_3I$  is initially unreactive with uranium. However, a  $CH_3$  radical, formed following a dissociative surface process for  $CH_3I$ , would be more reactive than  $CH_4$ . Thus, we suggest that the iodine atom of  $CH_3I$  is selectively adsorbed on uranium and forms a sublayer of  $UI_3$ . Following this, uranium could react with the  $CH_3$  radicals to produce

uranium carbide liberating hydrogen (equation 3) or producing uranium hydride (equation 2). In this scheme an overlayer of carbide carbon would result. To evaluate this suggestion XPS spectra were measured at an electron take-off angle  $\phi = 80^\circ$  and compared with spectra obtained at  $\phi = 10^\circ$ . Defining the enhancement ratio ER as

$$ER = \frac{(A/S)_{\phi = 80^\circ}}{(A/S)_{\phi = 10^\circ}} \quad (4)$$

with  $A/S$  = adsorbate to substrate atomic ratio and

$\phi$  = electron take-off angle, relative to the surface normal

one would expect ER to be significantly greater than 1 if an adsorbate overlayer is formed. The enhancement ratio for I/U would not be expected to change to the same extent for a sub-surface iodine species. The enhancement ratios were determined to be 2.8 and 2.6 for carbon and 1.8 and 1.9 for iodine at  $\text{CH}_3\text{I}$  exposures of 0.5 and 5.0 L, respectively. The individual ratios for each exposure are equal within the experimental precision ( $\pm 0.4$ ). While the precision of these measurements on polycrystalline materials is not high and although our own results are limited by the low amount of carbon and iodine adsorbed on uranium, the relative ER values for carbon and iodine suggest that carbon is indeed more concentrated in an outer surface layer. This finding is consistent with the notion that a uranium iodide sublayer is formed in the initial adsorption reaction.

### 3.2.4 Kinetics

The changes in atomic and intensity ratios (after conversion to the fractional coverage  $\theta$ ) as a function of  $\text{CH}_3\text{I}$  exposure were examined to investigate the kinetics of adsorption. The term  $\theta$  represents an experimental fractional coverage which can be evaluated from the measured iodine to uranium or carbon to uranium intensity ratios by setting the value of  $\theta = 1$  at saturation. Saturation occurred at about 2.0 L for  $\text{CH}_3\text{I}$  adsorption on uranium. At saturation on uranium the atomic ratios are  $I/U$  (XPS) = 0.3 and  $C/U$  (XPS) = 0.09. In the graphs in Fig. 8 and Fig. 9 for the I/U and C/U results, respectively, a linear increase of the ratios is observed up to values corresponding to  $\theta = 0.6 - 0.7$  for both sets of data and for ratios calculated from XPS and AES measurements. Such a linear behavior is indicative of a coverage independent sticking coefficient. Because of potential errors in recording the pressure using an uncalibrated ionization gauge, the evaluation of sticking coefficients was not carried out.

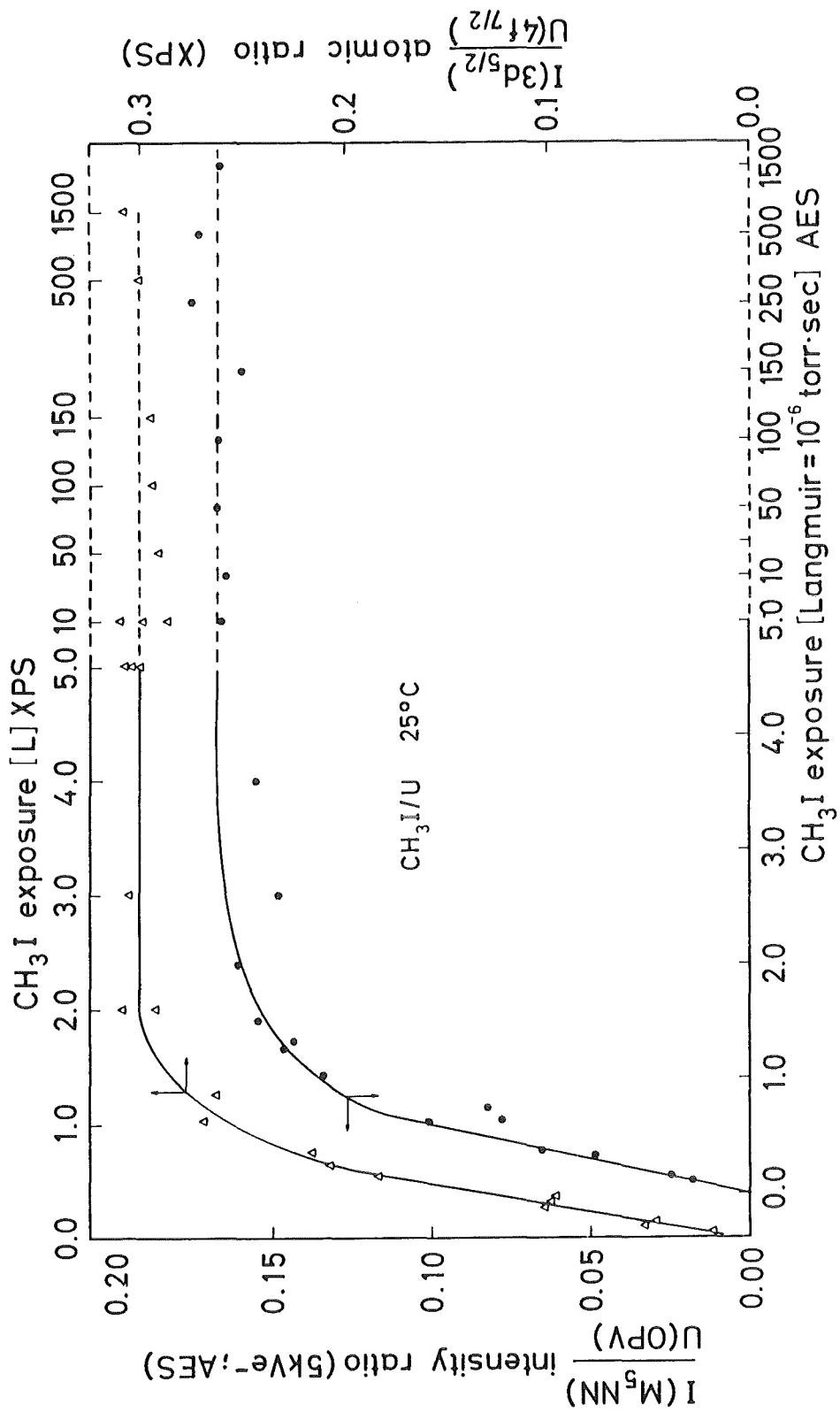


Fig. 8: I/U: XPS (atomic) and AES (intensity) ratios as a function of CH<sub>3</sub>I exposure on uranium

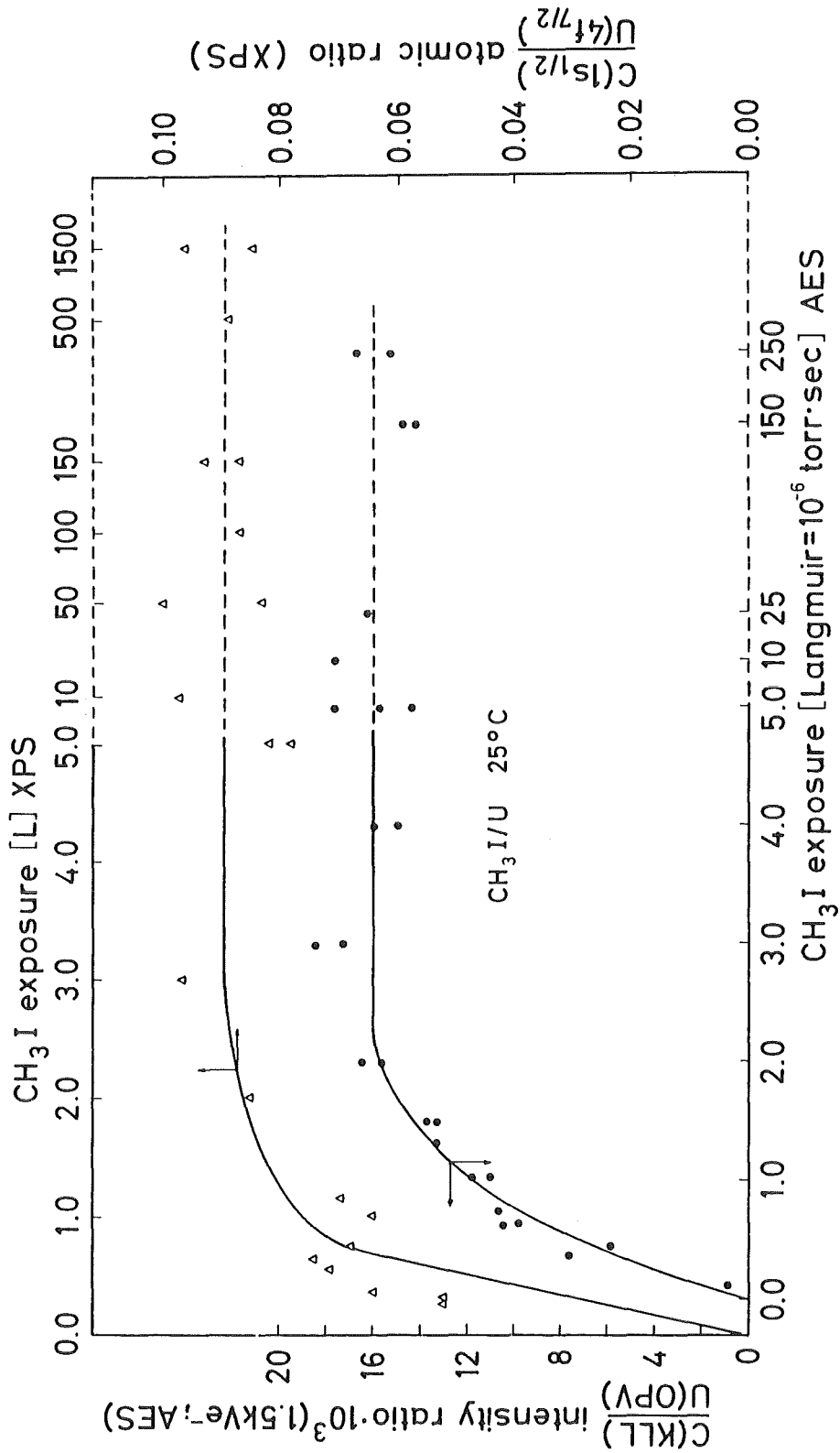


Fig. 9: C/U: XPS (atomic) and AES (intensity) ratios as a function of CH<sub>3</sub>I exposure on uranium

The application of different kinetic models (51) leads to different functional changes  $f(\theta)$  vs. exposure. Since a dissociative adsorption process is supported by the spectral measurements, it could be anticipated that second order kinetic behavior in the fraction of unoccupied sites would be observed (51-53). A plot of the function  $f(\theta) = \frac{\theta}{1-\theta}$  vs coverage for I/U is shown in Fig. 10. The  $f(\theta)$  results were obtained from XPS and AES data, and it is evident that the data points show equivalent functional behavior. However, a linear functionality for  $f(\theta)$ , as would be expected for second order kinetics, is not found.

The observation of constant sticking probability is believed (54,55) to be indicative of a precursor state (52,53). In this model the initially adsorbed molecule exists as a weakly adsorbed, short-lived species which is insensitive to surface coverage and mobile enough to seek out final bonding/adsorption sites. In treating our results, we have taken the simplest form of the precursor model as a starting point. Following the treatment developed by Kisliuk (52) and applied to adsorption on transition metal surfaces (51,53), we show in Fig. 11 a plot of  $f(\theta) = c\theta - (1-c)\ln(1-\theta)$ ,  $c = 0.45$ , for the I/U AES results. Although the data points are somewhat scattered, a reasonable fit to a precursor model is demonstrated. Other reasonable fits of the data could be obtained for  $c$  in the range of 0.4 - 0.5.

In comparing the adsorption of diatomic halogens on Fe(100) (55), an increased lifetime in the precursor state was found proceeding from chlorine to bromine to iodine. This change was explained (55) by an increased Van der Waals attraction at the surface for the larger, more polarizable iodine molecule. For adsorption of the polar  $\text{CH}_3\text{I}$  molecule it is probable that dipolar attractive forces determine the lifetime of the precursor state and the orientation of  $\text{CH}_3\text{I}$  on the surface. If the idea of uranium-iodine bond formation in the initial adsorption step is combined with the finding that first order kinetics are observed, the result implies that iodine-uranium bond formation is rate controlling. Thus the adsorption of  $\text{CH}_3\text{I}$  on an appropriate site, after whatever random sojourn the molecule has taken to find the site, is rate controlling and dissociation of carbon in some form, presumably  $\text{CH}_3$ , follows in a later step. An additional implication of 1) the kinetic data, 2) the angular dependence results, and 3) the suggestion of the formation of a sub-surface iodide layer would be that termination of the adsorption process occurs when sufficient uranium sites are occupied and formation of the initial  $\text{U}\dots\text{I}-\text{CH}_3$  species is prevented.

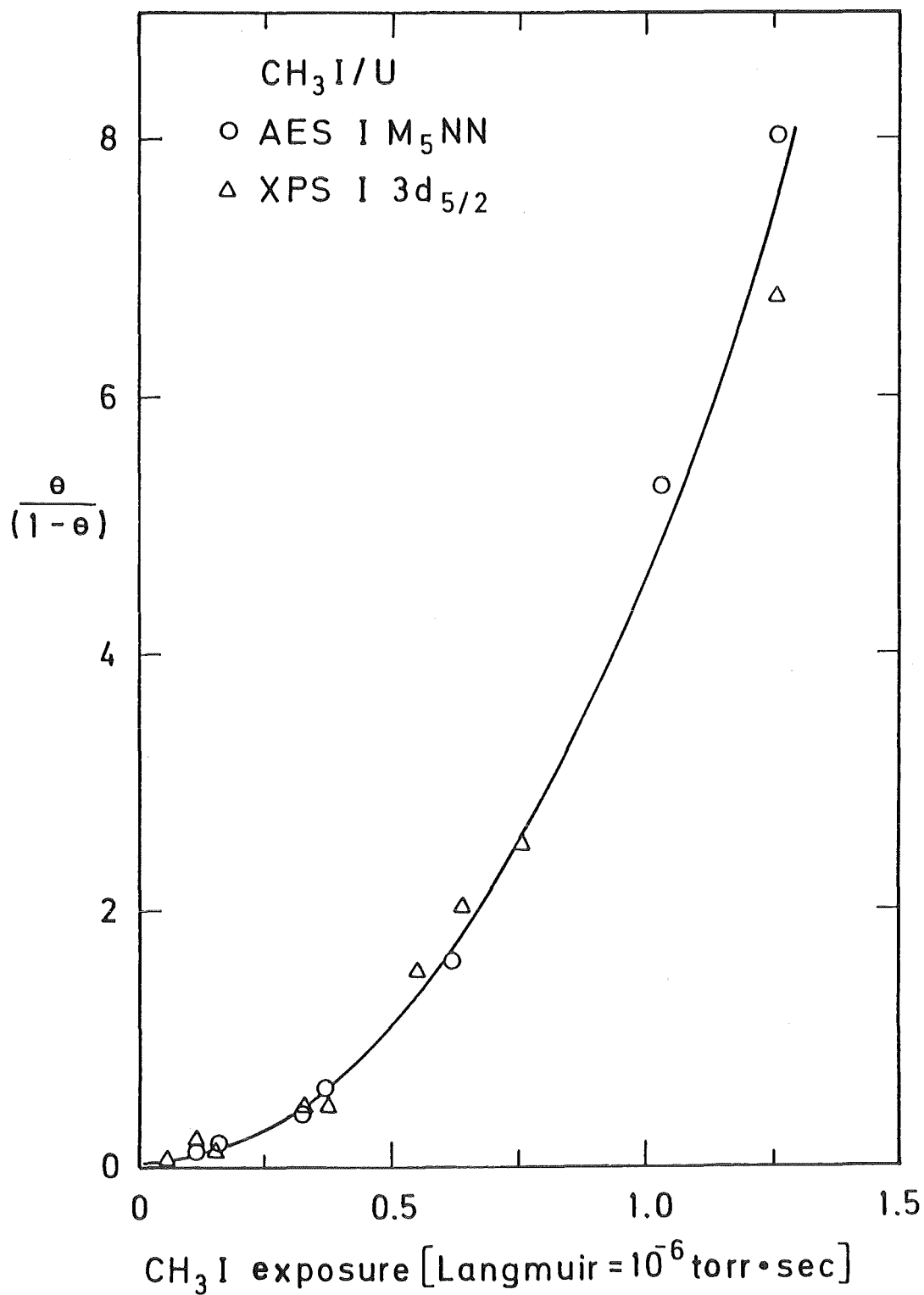


Fig. 10: CH<sub>3</sub>I adsorbed on uranium: second order kinetic plot,  $f(\theta) = \frac{\theta}{1-\theta}$   
(Evaluated from I/U XPS (atomic) and AES (intensity) ratios.)

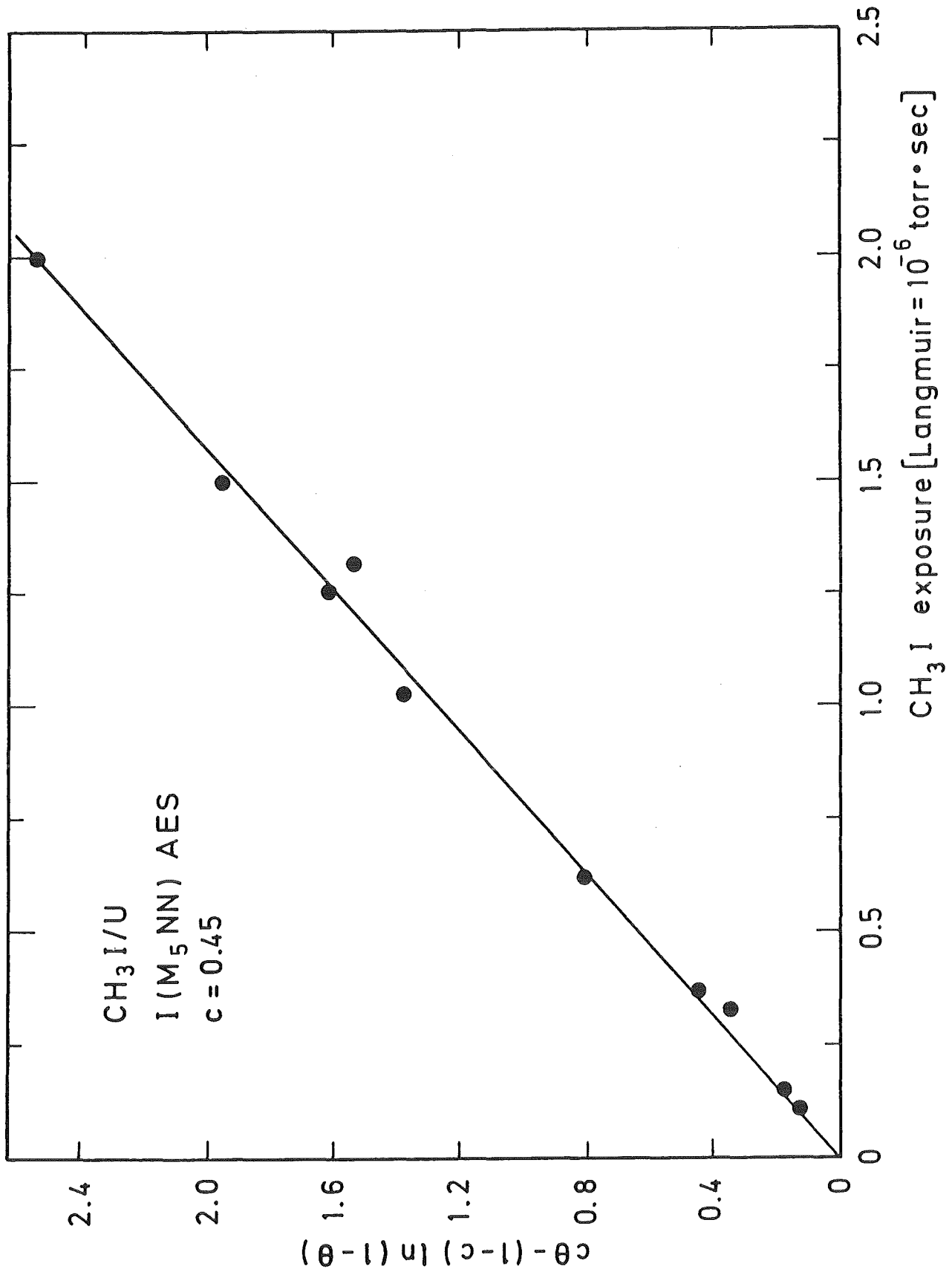


Fig. 11: CH<sub>3</sub>I adsorbed on uranium: First order kinetic plot-precursor model;  $f(\theta) = c\theta - (1-c) \ln(1-\theta)$   $c = 0.45$ . (Evaluated from I/U XPS (atomic) and AES (intensity) ratios.)

Although we have no direct proof of a mechanism, the results favor a reaction where  $\text{CH}_3\text{I}$  adsorption via uranium-iodine bonding occurs and that such an interaction is facilitated by dipole interactions with the uranium surfaces. Following uranium-iodine bond formation carbon is lost as  $\text{CH}_3$  and can adsorb subsequently to produce  $\text{UH}_3$  and  $\text{UC}$  or combine with hydrogen or  $\text{UH}_3$  to produce methane. Depending on the relative rates for iodine and carbon incorporation into uranium the initial behavior of  $f(\theta)$  vs exposure could indicate a difference in these rates. Unfortunately, because of the low carbon XPS and AES signals, our results are not sufficiently precise to distinguish whether the rates are in fact unequal. Realistically, the confirmation of any mechanism or model for  $\text{CH}_3\text{I}$  adsorption on uranium must rely on further studies using additional structural surface characterization techniques and comparative surface reactivities of uranium carbide, hydride, and iodide. Discussion of these topics is beyond the scope of this paper.

### 3.3 Adsorption of $\text{CH}_3\text{I}$ on $\text{UO}_2$

Adsorption of  $\text{CH}_3\text{I}$  on uranium dioxide was studied for exposures up to 1000 L. Spectroscopic results are presented only for XPS measurements because of interferences in the Auger transitions for iodine ( $\text{M}_4\text{N}_{4,5}\text{N}_{4,5}$ ), ( $\text{M}_5\text{N}_{4,5}\text{N}_{4,5}$ ) and  $\text{O}(\text{KLL})$  at  $\sim 515$  eV (KE) and of  $\text{C}(\text{KLL})$  and  $\text{U}(\text{NOV})$  at  $\sim 274$  eV (KE). Selected binding energy results for  $\text{U } 4f_{7/2}$ ,  $\text{I } 3d_{5/2}$  and  $\text{C } 1s$  at various  $\text{CH}_3\text{I}$  exposures are summarized in Table 2. No changes are detected in binding energy or peak shape as a function of coverage following adsorption of  $\text{CH}_3\text{I}$  on  $\text{UO}_2$ . Only one binding energy result is shown for carbon at a  $\text{CH}_3\text{I}$  exposure of 50 L because the quantity of  $\text{CH}_3\text{I}$  adsorbed is low and the subsequent  $\text{C } 1s$  signal is just above the XPS detection limit. In Fig. 12 we show XPS spectra in the  $\text{U } 4f$ ,  $\text{I } 3d$  and  $\text{C } 1s$  regions for clean  $\text{UO}_2$  and following saturation adsorption of  $\text{CH}_3\text{I}$ , respectively. The XPS results for carbon on  $\text{UO}_2$  (Fig. 12) were obtained by scanning the  $\text{C } 1s$  region for 15 hours at 100 watts X-ray power using a Mg anode. The  $\text{C } 1s$  spectrum for clean  $\text{UO}_2$  in Fig. 12 was obtained under experimental conditions identical to those following  $\text{CH}_3\text{I}$  exposure to  $\text{UO}_2$ . A comparison of the spectra in Fig. 12 demonstrates that the carbon signal, which was observed following  $\text{CH}_3\text{I}$  exposure, did not arise from adsorption of background carbon-containing gases. Although the  $\text{C } 1s$  FWHM (2.3 - 2.4 eV) is greater than that recorded for the  $\text{C } 1s$  peak for carbide carbon, a precise determination of the peak width is hampered by the low intensity of the photopeak. If the measured peak width is

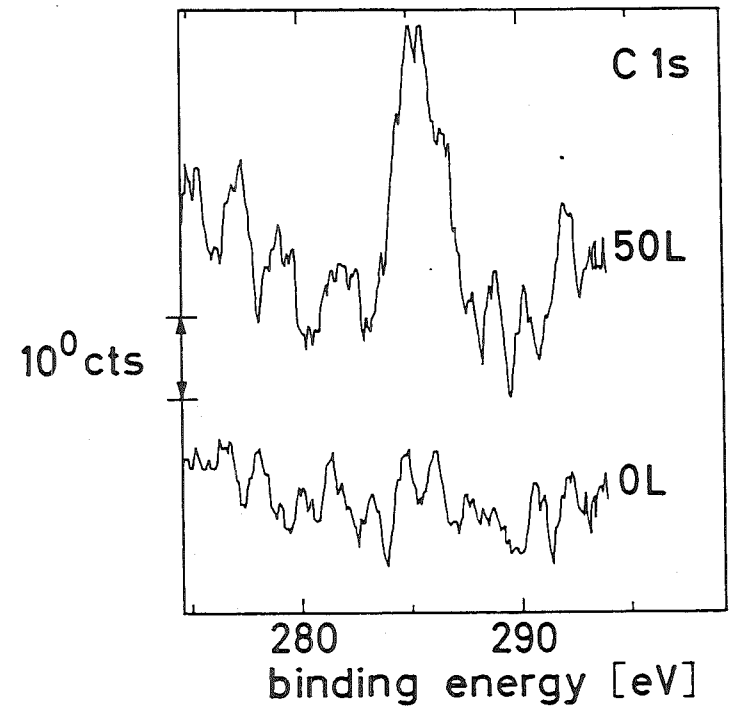
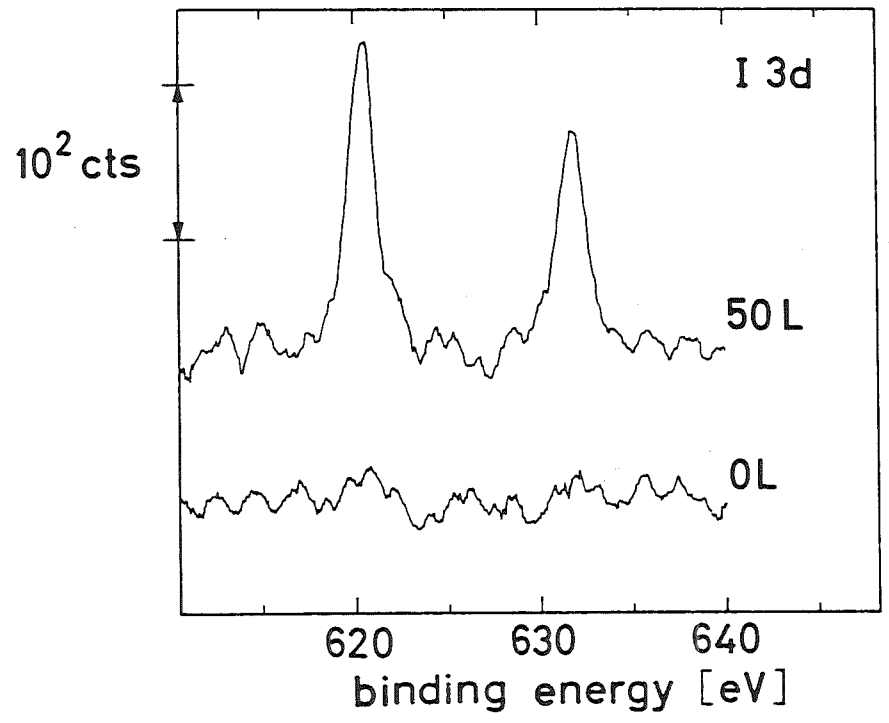
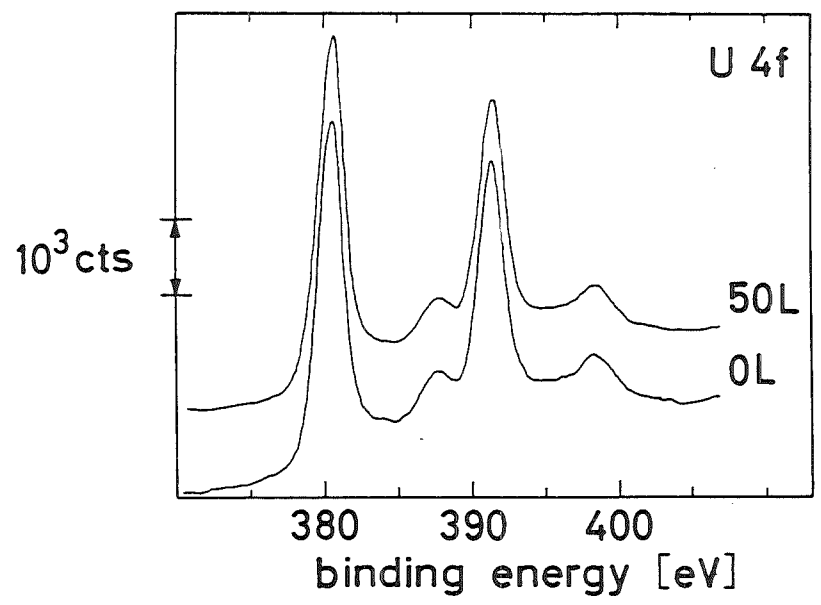


Fig. 12: X-ray photoelectron spectra (Mg anode) for clean uranium dioxide and following exposure to 50 L CH<sub>3</sub>I

accepted as reasonable, then the value could be interpreted to suggest that more than one carbon species is present on the  $\text{UO}_2$  surface. Our measurements for the very low intensity C 1s photopeak are not precise enough to speculate further on this point. For the following discussion we accept the C 1s binding energy and peak width as indicative of only one carbon type. The binding energy for carbon is clearly not equal to that noted for carbide carbon and is in the region characteristic of hydrocarbon type carbon at 285 eV (24). In addition, the binding energy difference  $\Delta E$  ( $\text{I } 3d_{5/2}$  - C 1s), 335.0 eV, is very near the value reported for gaseous  $\text{CH}_3\text{I}$  (31). These results could be interpreted to indicate a non-dissociative adsorption process for  $\text{CH}_3\text{I}$ . Alternatively, the difference in binding energies could arise if  $\text{CH}_3\text{I}$  were dissociatively adsorbed and formed bonds with surface atoms that altered the electron density at carbon and at iodine to the same extent. Likely species for forming such bonds are surface oxygen atoms. The reaction would yield U-O-I and U-O- $\text{CH}_3$  surface groups. The formation of these species in the reaction with electronegative oxygen could satisfy the finding that no change in  $\Delta BE$  ( $\text{I } 3d_{5/2}$  - C 1s) occurs.

At saturation the C/U and I/U atomic ratios are 0.03 and 0.034, respectively. We note that the I/C ratio is approximately 1.1. Because of the potential errors in measuring the adatom intensities, we take this value to be equal to 1.0 which indicates a 1:1 ratio of iodine to carbon on the surface. The I/C ratio is consistent with either dissociative or non-dissociative adsorption.

The XPS I/U atomic ratio, following thermal treatment at 600 °C of  $\text{UO}_2$  exposed to 1000 L  $\text{CH}_3\text{I}$  at 25 °C, showed no measurable change as shown in Fig. 7. For reasons mentioned previously carbon spectra were not measured after the thermal treatment. We presume that the absence of a significant change in the I/U ratio would also be found for the C/U ratio. This reasoning is based on the following:

1. if non-dissociative adsorption occurs, the alterations in the I/U and C/U ratios should parallel one another, and
2. if dissociative adsorption takes place, we expect the U-O-I interaction to be weaker than that for U-O- $\text{CH}_3$  (21), and thus no change in the I/U ratio would also suggest no change in the C/U ratio.

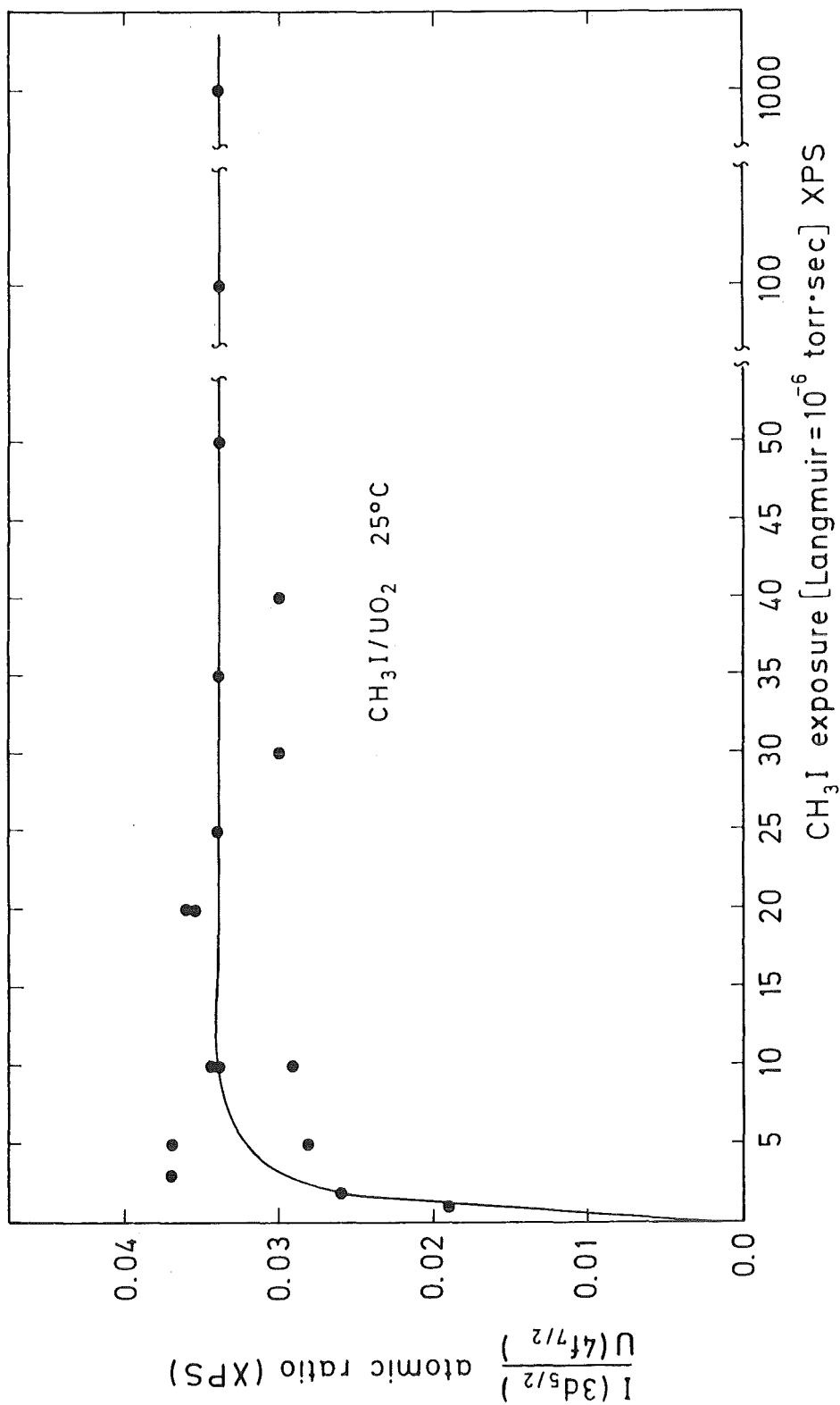


Fig. 13: I/U: XPS (atomic) ratio as a function of CH<sub>3</sub>I exposure on uranium dioxide

The thermal behavior of iodine ( $\text{CH}_3\text{I}$ ) adsorbed on  $\text{UO}_2$  is distinctly different from the corresponding behavior for iodine ( $\text{I}_2$ ) adsorbed on  $\text{UO}_2$  (see sect. 3.5.2). Iodine ( $\text{I}_2$ ) adsorbed on  $\text{UO}_2$  is desorbed almost completely following thermal treatment at  $600^\circ\text{C}$  in contrast to the behavior of iodine in  $\text{CH}_3\text{I}$  adsorption. Spectroscopic (XPS and AES), thermal stability, and kinetic results indicated a non-dissociative adsorption of iodine ( $\text{I}_2$ ) on  $\text{UO}_2$ . As a result of the significant differences in thermal stability for iodide ( $\text{CH}_3\text{I}$ ) adsorbed on  $\text{UO}_2$ , we suggest that a dissociative process occurs. However, no further experimental evidence was obtained regarding the surface species formed.

In Fig. 13 we show the adsorption behavior of  $\text{CH}_3\text{I}$  vs exposure as measured by the I/U XPS atomic ratio. The error in the precision of determining the ratio is about 15 %. The curve was generated to establish the I/U ratio at saturation and the exposure at which saturation occurs. In the exposure range 2-10 L the curve presented in the figure is thought to be the best representation of  $f(\theta)$ . Above 10 L the majority of the data points indicate that saturation has occurred. Based on the limited data the variation in I/U is drawn as a linear function in the exposure range 0-2 L. The point at which the line becomes non-linear is at  $\text{I}/\text{U} = 0.026$  which corresponds to  $\theta = 0.76$ . The presumed linear variation would suggest precursor state kinetic behavior as discussed above for uranium metal. The present results are not amenable to any kinetic treatment in order to establish the order of the adsorption reaction.

### 3.4 Adsorption of Molecular Iodine on Uranium Metal

Adsorption of molecular iodine on clean uranium ultimately leads to the formation of a uranium iodide surface. Binding energy results (XPS) and Auger kinetic energy data measured as a function of  $\text{I}_2$  exposure are summarized in Table 3. Valence and U 4f regions in the XPS spectra at selected  $\text{I}_2$  exposures are shown in Figs. 14 and 15, respectively. A change in the photopeak shape is recorded for the valence band spectra shown in Fig. 14. A clean uranium spectrum shows no evidence of the uranium-ligand band in the 3 to 6 eV range which has been studied for uranium oxides (3,4,9) and halides (37). With increasing  $\text{I}_2$  exposure a uranium-iodine (U-I) band at  $\approx 4$  eV increases in intensity and at saturation ( $\approx 40$  L  $\text{I}_2$ ) is clearly separated from the U 5f peak. The spectrum shown in Fig. 14 for 100 L  $\text{I}_2$  exposure is identical to the one obtained for an exposure of 40 L  $\text{I}_2$ . Exposure of uranium to  $\text{I}_2$  also results in the appearance of the I 5s photopeak at 17 eV, and there is a shift in the U 5f peak

Table 3: ENERGETIC RESULTS: XPS and AES for I<sub>2</sub> adsorption on Uranium and Uranium Dioxide

I <sub>2</sub> Exposure (L)	XPS BINDING ENERGY			AES KINETIC ENERGY			
	U 4f <sub>7/2</sub> (±0.1 eV)	U 4f <sub>5/2</sub> (±0.1 eV)	I 3d <sub>5/2</sub> (±0.1 eV)	O 1s (±0.1 eV)	I(M <sub>4</sub> N <sub>4,5</sub> N <sub>4,5</sub> ) (±0.3 eV)	I Auger para- meter α (eV)	U(OPV) (±0.5 eV)
Uranium metal							
0	377.4	-	-	-	-	-	74.4
0.064	377.4	-	620.4	-	518.8	1139.2	74.4
0.079	377.4	-	620.3	-	519.1	1139.4	74.3
0.15	377.4	-	620.3	-	519.1	1139.4	74.1
0.32	377.4	-	620.2	-	518.6	1138.8	73.5
0.39	377.4	-	620.2	-	518.7	1138.9	73.9
1.0	377.3	379.0	620.2	-	518.1	1138.3	72.5
1.2	377.3	379.0	620.3	-	517.9	1138.2	71.8
1.9	377.4	379.0	620.3	-	517.6	1137.9	72.1
2.9	377.4	378.9	620.2	-	517.7	1137.9	70.8
3.9	377.4	378.9	620.3	-	517.5	1137.8	71.0
4.2	377.4	379.0	620.3	-	517.4	1137.7	70.6
5.2	377.4	379.0	620.3	-	517.3	1137.6	70.5
6.4	377.4	379.0	620.3	-	517.2	1137.5	70.5
11.3	377.3	378.9	620.3	-	517.1	1137.4	70.9
39.7	377.3	379.0	620.4	-	517.0	1137.4	70.6
51.3	377.3	379.0	620.3	-	517.1	1137.4	70.9
60.3	-	379.0	620.4	-	517.0	1137.4	70.9
100.0	-	379.0	620.3	-	517.2	1137.5	70.8
Uranium dioxide							
0	380.5	-	-	530.5	-	-	72.6
0.05	380.5	-	620.1	530.6	-	-	73.0
0.10	380.4	-	620.0	530.4	-	-	72.7
0.30	380.5	-	619.6	530.5	518.0	1137.6	72.9
0.50	380.4	-	619.6	530.5	518.1	1137.7	72.5
1.0	380.5	-	619.5	530.5	517.6	1137.1	72.9
1.6	380.5	-	619.5	530.6	517.4	1136.9	73.3
4.0	380.4	-	619.5	530.4	517.9	1137.4	72.5
5.7	380.5	-	619.6	530.5	517.4	1137.0	72.5
15.5	380.4	-	619.4	530.5	517.2	1136.6	NM
29.0	380.5	-	619.6	530.5	516.6	1136.2	72.7
41.3	380.5	-	619.5	530.5	516.4	1135.9	72.9
51.3	380.5	-	619.7	530.5	516.5	1136.2	72.7
75.0	380.5	-	619.6	530.5	516.8	1136.4	72.9
I <sub>2</sub> (s)	-	-	619.9	-	519.0	1138.9	-
I <sub>2</sub> (s) <sup>a</sup>	-	-	620.5(±0.2)	-	-	-	-
I <sub>2</sub> (s) <sup>b</sup>	-	-	619.9	-	-	-	-
CH <sub>3</sub> I/UO <sub>2</sub> <sup>c</sup>	-	-	620.3	-	-	-	-

NM = not measured

a) = Ref. 38, 39

b) = Ref. 45

c) = Ref. 35 and sect. 3.3

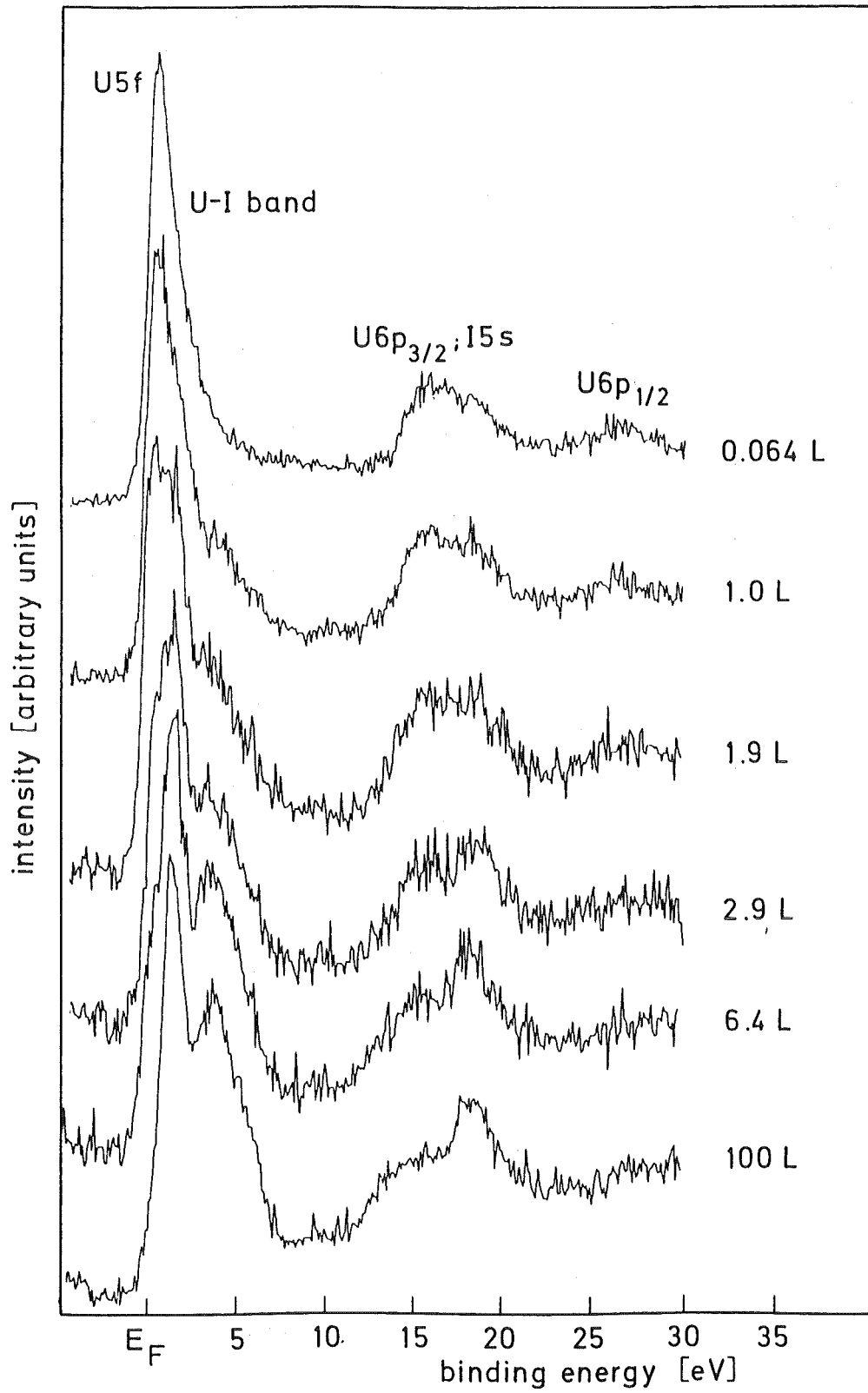


Fig. 14: XPS spectra of valence region as a function of I<sub>2</sub> exposure (1 L = 10<sup>-6</sup> torr · sec)

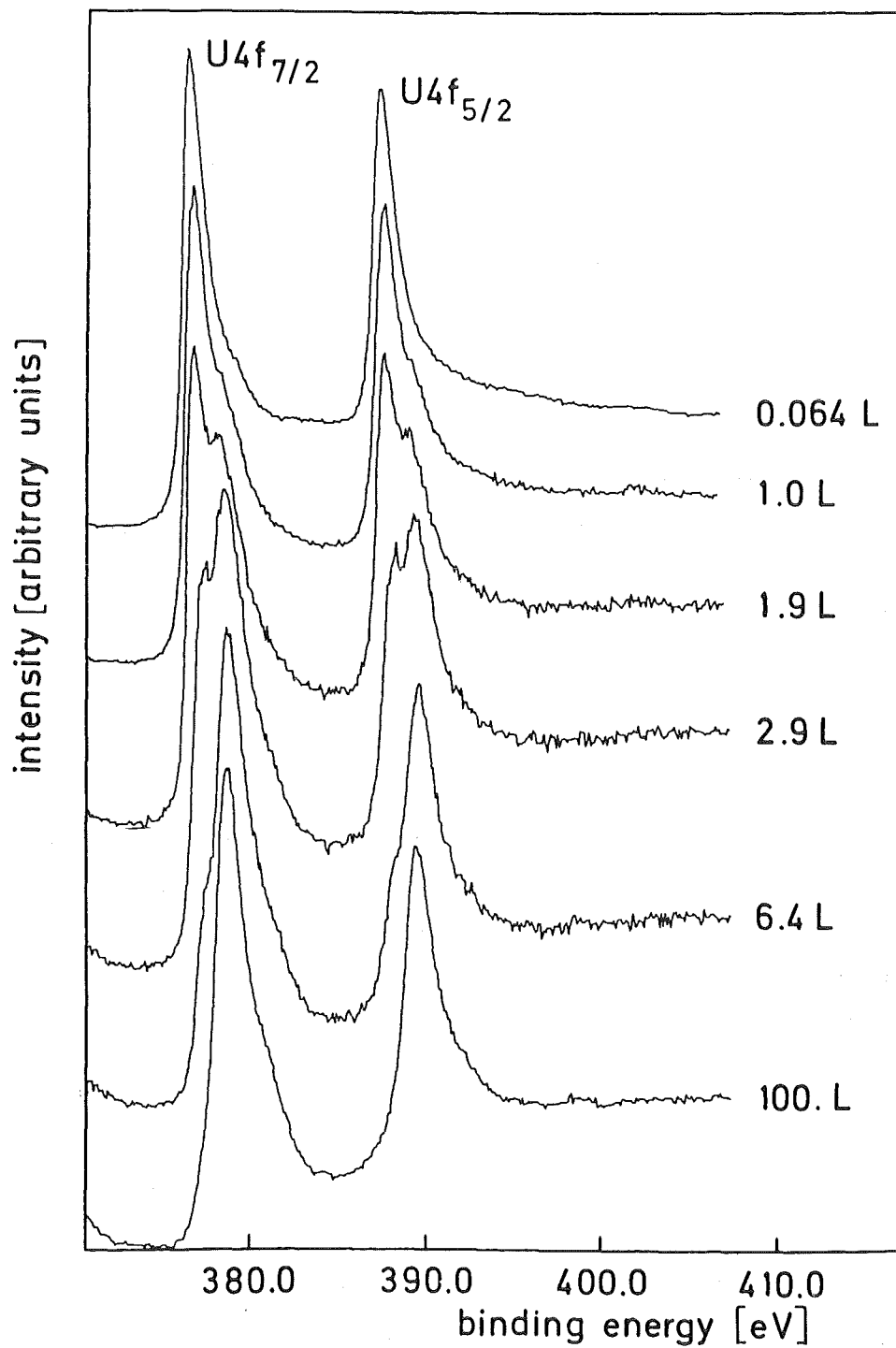


Fig. 15: U 4f XPS spectra as a function of I<sub>2</sub> exposure (1 L = 10<sup>-6</sup> torr · sec)

maximum to about 2.0 eV below the Fermi level. This corresponds to a shift of about 1.5 eV for the U 5f peak maximum in going from uranium metal to uranium iodide.

The uranium 4f spectra at selected I<sub>2</sub> exposures are shown in Fig. 15. The spectrum for 0.064 L I<sub>2</sub> exposure is equivalent to the spectrum recorded for clean uranium. The slight shoulder on the high binding energy side of the U 4f<sub>7/2</sub> peak is due to the Mg X-ray satellite from U 4f<sub>5/2</sub> which was not removed before plotting these spectra. The absence of a shoulder on the high energy side of the U 4f<sub>5/2</sub> peak shows that no uranium species with a binding energy greater than that for the pure metal is present. However, for exposures beginning at 1.0 L I<sub>2</sub> and continuing to saturation at about 40 to 50 L I<sub>2</sub>, the U 4f photopeaks each show evidence for at least two uranium species. The recorded spectra show a decreasing contribution by the uranium metal photopeaks. At 40 L iodine exposure the U 4f spectra indicate that the uranium metal content is less than about 5 % (atomic). The five percent uranium content is the concentration at which uranium metal photopeaks just could be curve resolved from a peak envelope containing photopeaks attributable to uranium metal and a uranium iodide.

In the curve resolution analysis of the U 4f<sub>7/2</sub> photopeak envelope it was possible to obtain three components: one attributable to uranium metal at a binding energy (BE) of 377.4 eV, a second peak at BE = 379.0 eV, and a third component at 380.9 eV. A typical fit of the U 4f<sub>7/2</sub> photopeak for an I<sub>2</sub> exposure at 11.3 L is shown in Fig. 16. We attribute the main U 4f<sub>7/2</sub> photopeak at 379.0 eV to a uranium iodide and the smaller peak at 380.9 eV to a shake-up satellite feature (24) rather than to another uranium iodide species (37). Support for this assignment comes from the additional consideration of the stoichiometric I/U ratio at saturation.

The variations in the iodine to uranium absolute atomic ratio (XPS) and the iodine (M<sub>5</sub>N<sub>4,5</sub>N<sub>4,5</sub>) to uranium (OPV) peak intensity ratio (AES) are shown in Fig. 17 as a function of I<sub>2</sub> exposure. The exposure scale for the AES results is offset in the figure for clarity; the ratios at low exposures are shown in the inset. The absolute atomic ratio for I/U at saturation is 3.04. This result indicates that a UI<sub>3</sub> surface is formed in the reaction with iodine and that the adsorption process for I<sub>2</sub> is dissociative. Thermal treatments of the I<sub>2</sub> saturated uranium surface were carried out to aid in confirming the formation of UI<sub>3</sub> and

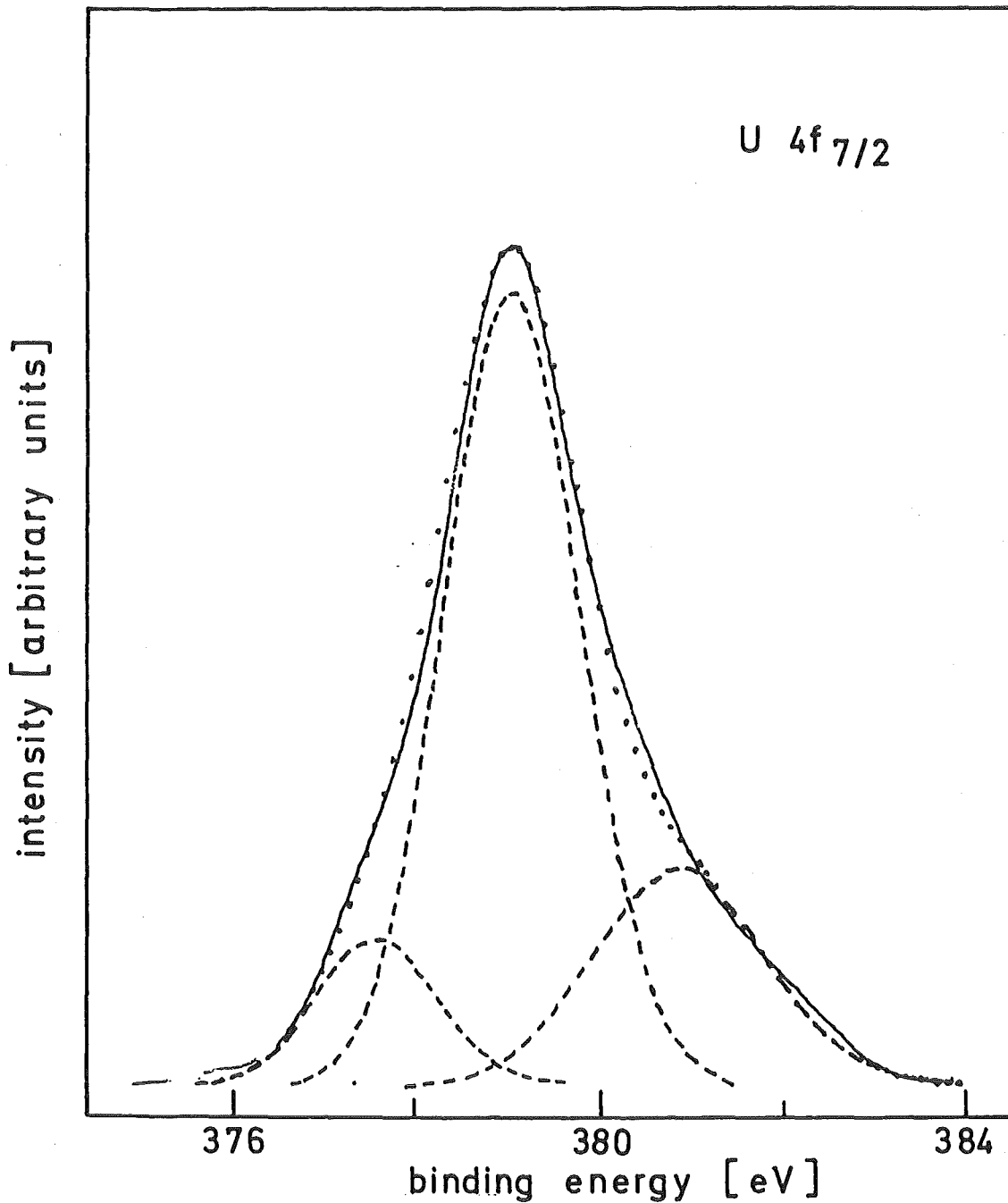


Fig. 16: Multiplet analysis of the U 4f<sub>7/2</sub> photopeak for an exposure of 11.3 L (1 L = 10<sup>-6</sup> torr · sec) I<sub>2</sub> on uranium metal (solid curve: experimental multiplet; dotted curve: fitted multiplet; dashed curves: resolved components). The analysis was carried out after removal of the X-ray satellite of the U 4f<sub>5/2</sub> photopeak (main component: U I<sub>3</sub>; left component U metal; right component: U I<sub>3</sub> satellite)

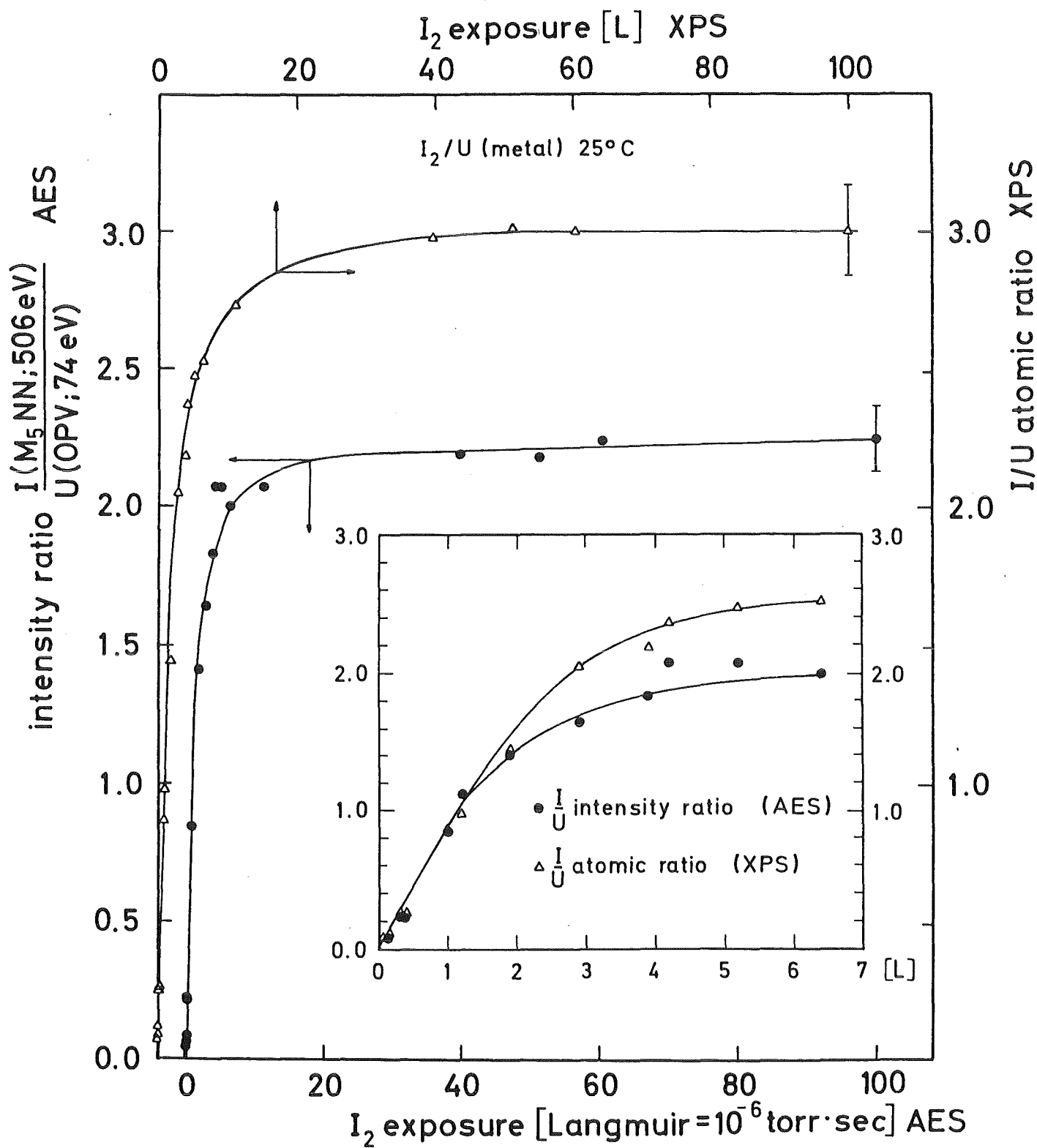


Fig. 17: AES intensity ratio and XPS atomic ratio vs.  $I_2$  exposure on uranium metal. The inset shows an expansion of the low exposure region

eliminating the possibility of the presence of higher iodides,  $UI_4$  or  $UI_5$ . The results are presented in Fig. 18 where the I/U XPS atomic ratio for two different thermal treatments following two different  $I_2$  exposures are shown. The I/U atomic ratios and the absolute photopeak intensities do not change following the thermal treatment. The vapor pressure behavior of  $UI_4$  has been investigated (22) and a vapor pressure of about 200 torr is calculated at 600 °C. Such a high vapor pressure for the duration of our thermal studies would lead to sublimation of  $UI_4$  and loss of iodine photopeak intensity. We observe no significant loss of iodine signal and no significant change in the I/U atomic ratio. These findings demonstrate that  $UI_4$  is not present and support our contention that  $UI_3$  is formed. Although vapor pressure data are not available (22) for  $UI_3$ , it is known that the volatility of  $UI_3$  is less than that of  $UI_4$ . However, the vapor pressure of any lower valent iodides,  $UI$  or  $UI_2$ , would also be expected to be lower than that for  $UI_4$ . We cannot exclude the presence of  $UI$  or  $UI_2$  surface phases based on the thermal studies alone. Nevertheless, the formation of  $UI$  or  $UI_2$  would be unexpected considering the known chemistry of uranium-iodine systems (21) and difficult to rationalize recognizing our measured I/U atomic ratio being equal to 3. We conclude that a single uranium iodide phase is produced,  $UI_3$ .

#### 3.4.1 Interpretation of XPS Binding Energies and AES Kinetic Energies

We interpret the XPS binding energy and AES kinetic energy results in a qualitative manner. Among the factors that contribute to the magnitude of the energies are the energies of initial and final states and relaxation contributions. Variations in relaxation energies resulting from chemical effects have been investigated experimentally and theoretically (29,30,44,63). In relaxation processes, atomic and extra-atomic electrons are polarized toward the core hole which is created upon ionizing a given core level. In the case of XPS ionization the core hole is singly charged, while for AES the final state is doubly charged. The shift of electron density toward the hole has the effect of neutralizing the atomic charge and thus lowers the binding energy and increases the kinetic energy of the ejected electrons. Since electron polarization is related to the magnitude of the final ion charge, the effect on the measured ejected electron kinetic energy is greatest for Auger processes where the final ion is doubly charged. In the following discussions it is believed that changes in the Auger kinetic energies for iodine as a function of iodine exposure arise from relaxation effects due to the substrate atoms.

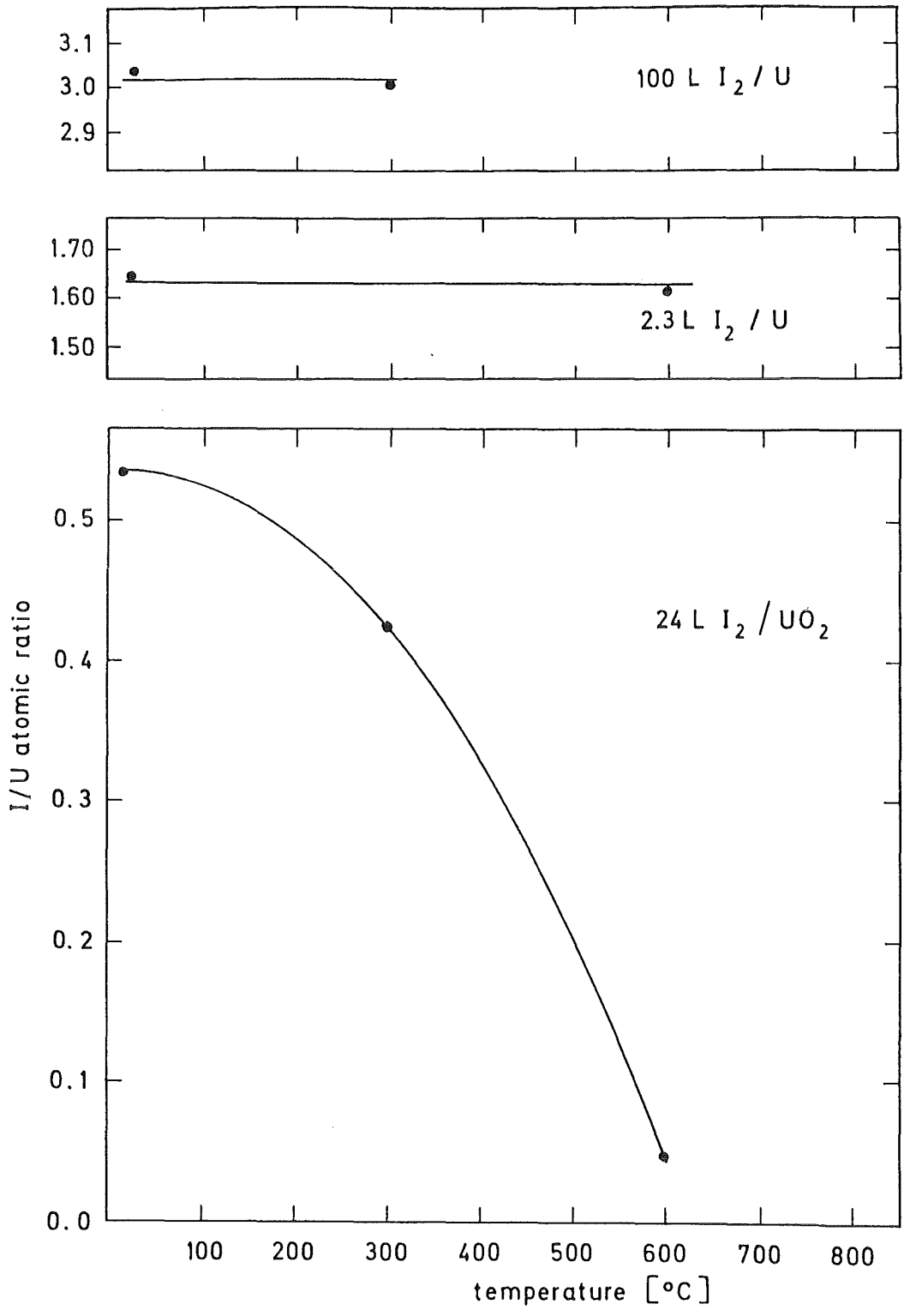


Fig. 18: Thermal desorption behavior of uranium and uranium dioxide surfaces after exposure to iodine

In the X-ray photoelectron study (37) for a number of uranium halides and oxyhalides of fluorine, chlorine, and bromine no measurements were conducted for iodides or oxyiodides. The reported (37) U 4f<sub>7/2</sub> binding energies for trihalides are UF<sub>3</sub>, 379.9 eV; UCl<sub>3</sub>, 378.1 eV; and UBr<sub>3</sub>, 378.2 eV. The U 4f<sub>7/2</sub> binding energy, measured in this study for UI<sub>3</sub>, 379.0 eV, appears high when compared to the other halides in the homologous series. However, it was remarked (37) that the spectra for UX<sub>3</sub> compounds could not be regarded as free from contamination, particularly by oxygen. In this study we do not detect oxygen in either the XPS or AES spectra following the preparation of the UI<sub>3</sub> surface. Thus, we regard the binding energies and the spectral features obtained in this study as characteristic of clean stoichiometric UI<sub>3</sub>. The presence of satellite structure in the U 4f spectra and particularly the satellite energy separation from the main peak of 1.9 eV seems reasonable in view of the expected higher covalency of the U-I bond (37,64). The satellite separation can be compared with separations in UBr<sub>4</sub>, 5.8 eV and UBr<sub>5</sub>, 2.8 eV. We select the bromides for comparison since they are expected to be more covalent than chlorides, but less covalent than iodides. The satellite separation in UI<sub>3</sub> is less than the value for the most covalent bromide, UBr<sub>5</sub>, and if we use satellite separations alone as a measure of covalency, this would lead to the suggestion that UI<sub>3</sub> is more covalent than UBr<sub>5</sub>. This picture is surely too simplified, but we anticipate that the trend in satellite separation for a given halogen in different oxidation states would vary UX<sub>3</sub> > UX<sub>4</sub> > UX<sub>5</sub>. The satellite separation measured for UI<sub>3</sub> would correspond to the greatest value expected for these uranium iodides. Further, the satellite intensity relative to the main photopeak is expected to vary in the manner UI<sub>n</sub> > UBr<sub>n</sub> > UCl<sub>n</sub> > UF<sub>n</sub> for a homologous halide series, and among uranium oxidation states the ratio should change as UX<sub>5</sub> > UX<sub>4</sub> > UX<sub>3</sub> (24,37). Thus the satellite intensity for UI<sub>3</sub>, approximately 40 % in relative intensity compared to the main peak, is expected to represent the maximum intensity in the series of uranium trihalides and minimum for UI<sub>n</sub> compounds.

Auger electron kinetic energies for the iodine M<sub>4</sub>N<sub>4,5</sub>N<sub>4,5</sub> (X-ray induced) and for the uranium OPV (electron induced) transitions were measured relative to the Fermi level to aid in identifying the chemical state of adsorbates by determining the Auger parameter (29). The Auger results are summarized in Table 3. The important result is the observed change in the kinetic energy of the iodine and uranium transitions as I<sub>2</sub> exposure increases. For the U(OPV) transition the change in energy is a direct result of converting uranium metal to a uranium triiodide surface. We expect the Auger spectra to be a composite

of the spectra for clean uranium and for uranium triiodide which is being formed even at low exposures in the initial stages of  $I_2$  adsorption. The shift of the U(OPV) electron kinetic energy to lower values for uranium iodide compared to uranium metal is similar to the shift observed for the uranium-uranium dioxide system (1). The lower energy arises from the fact that conversion of U(0) to U(III) results in a smaller energy separation between the electronic levels involved in the transition and a shift of the valence electrons to energies further below the Fermi level.

The shift in the iodine ( $M_4N_{4,5}N_{4,5}$ ) electron kinetic energy of about 2 eV with increasing  $I_2$  exposure may arise from extra-atomic relaxation processes. Since only one uranium iodide species,  $UI_3$ , is formed, we do not associate the kinetic energy shifts with the formation of different surface iodides. At low surface coverages iodine in  $UI_3$  is surrounded by unoxidized uranium atoms which can be a source of relaxation (30,44,63) for the doubly charged final ion. For the alteration of the iodine Auger kinetic energies we imagine that extra-atomic screening, which renders the iodine electrons in a more repulsive state, can be accomplished via the polarization of uranium metal valence electrons. Kowalczyk et al. (63) have shown for transition elements that unpaired electrons in d orbitals play an important role in relaxation processes. It was noted (63) that relaxation effects for early first row transition elements were greater than for copper and zinc since in these latter two elements the d orbitals are filled. The valence electrons in uranium are principally 5f electrons and are unpaired. These electrons are weakly bound with a binding energy of about 0.5 eV and could readily provide electron screening for iodine relaxation at low iodine coverage. As iodine coverage increases more uranium atoms are converted to uranium(III) species. In this process the availability of electron rich U(0) surface atoms decreases, and the extent of the relaxation effect is diminished. Thus we note a lower kinetic energy for the  $I(M_4NN)$  transition at higher  $I_2$  exposures. In principle, a similar variation but of lower magnitude should be found for I 3d binding energies as the surface coverage increases. The I 3d<sub>5/2</sub> binding energy is  $620.3 \pm 0.1$  eV at all exposures, and there is no trend in the binding energy results. We can offer no explanation as to why a recognizable shift in the Auger kinetic energies is observed, whereas no significant change in the I 3d<sub>5/2</sub> XPS binding energies is found.

The Auger parameter  $\alpha$  has been determined (44) for a series of transition metal fluorides and iodides. The change in the Auger parameter for halides with metals in different oxidation states and with different percentages of ionic bonding

character was spread over 0.5 eV for a series of transition metal iodides. This result demonstrates that the extra atomic relaxation energy contribution to anion electron binding energies is similar for a series of inorganic iodides. To compare the present results with those for simple iodides, which were quoted for the  $I(M_5N_{4,5}N_{4,5})$  transition, we add 11.5 eV to the values (44) to transform the results to correspond to the  $I(M_4N_{4,5}N_{4,5})$  data given here. The iodine Auger parameter range was 1137.3 to 1137.8 eV (44). That the  $\alpha$  value for  $UI_3$  at 1137.5 eV falls in the range for transition metal iodides reinforces the observation (44) that  $\alpha$  values in salts are little affected by changing the metal ion.

The electron induced Auger spectra for uranium transitions in the region 120-60 eV change dramatically with coverage as illustrated in Fig. 19. The spectra for exposures greater than 60 L are identical to the last spectrum shown in Fig. 19 which corresponds to  $UI_3$ . These spectra at high exposures indicate, as did the XPS spectra, that no further surface chemical changes are apparent. The spectra produced following exposure in the range 1.0 to 2.9 L  $I_2$  can be regarded as composed of various contributions from U and  $UI_3$  surfaces. That a  $UI_3$  species is produced at low exposures can be demonstrated by evaluating the stoichiometry of the iodide species using the integrated peak intensities of the I 3d photopeak and of the uranium component at 379.0 eV ( $UI_3$ ) including the satellite at 380.9 eV ( $UI_3$ ) in the U 4f<sub>7/2</sub> multiplet. To do this we assume

- 1) that the iodide layer is uniform;
- 2) that the U 4f XPS spectra can be represented as a combination of uranium metal and uranium triiodide from which each uranium component can be resolved;
- 3) that iodide is present and is associated only with uranium represented by the high binding energy photopeaks; and
- 4) that any error attributable to differences in the I 3d (BE  $\approx$  620 eV) and the U 4f (BE  $\approx$  380 eV) electron mean free paths is included in the empirically determined sensitivity factor.

The I/U atomic ratio of the uranium iodide species calculated for each exposure in the range 0.4 to 11.3 L  $I_2$  is  $3.1 \pm 0.2$ . Considering the assumptions made and the accuracy of the curve resolved fit to the U 4f peak envelope, the agreement

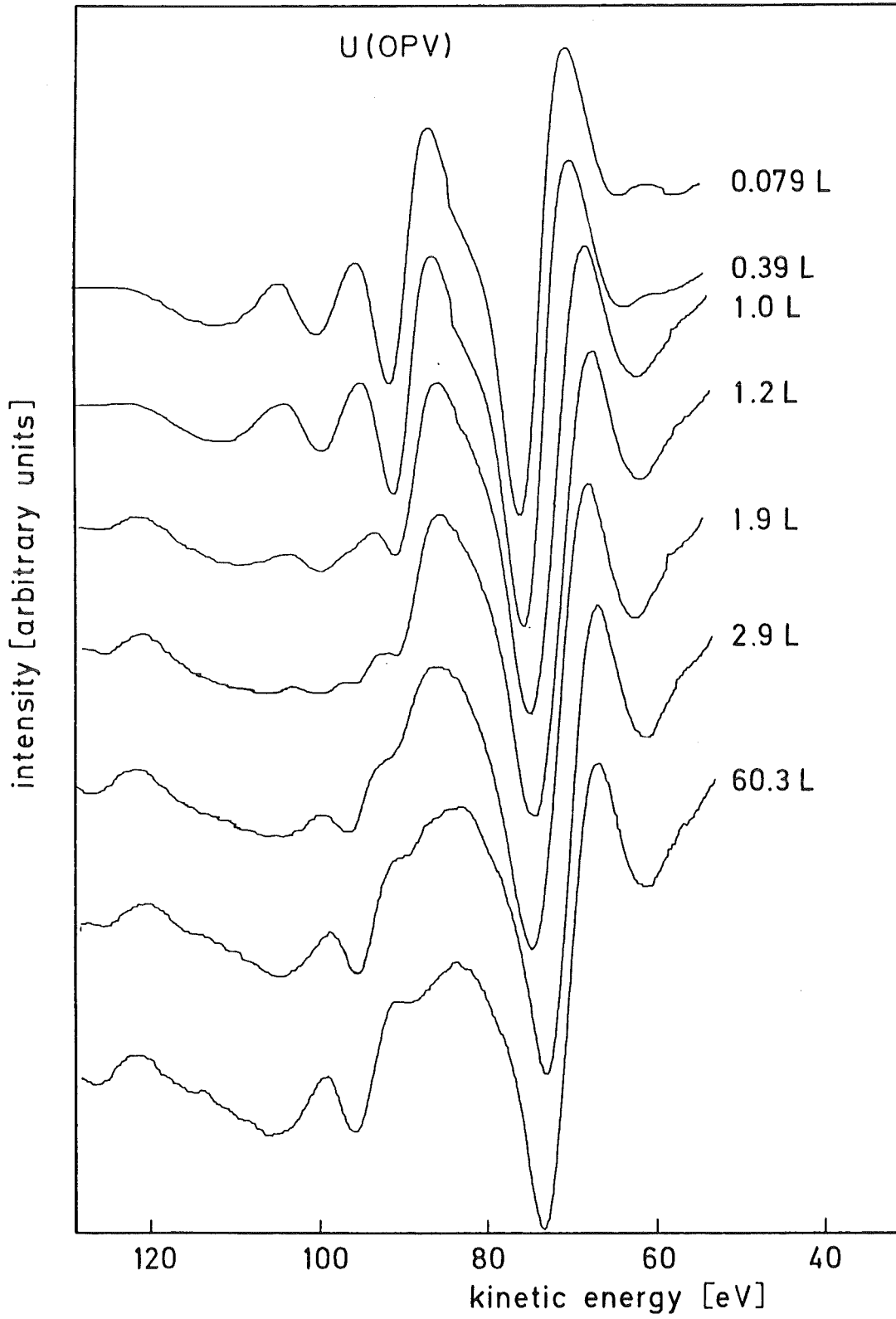


Fig. 19: U(OPV) AES spectra in the low kinetic energy region as a function of I<sub>2</sub> exposure (1 L = 10<sup>-6</sup> torr · sec) on uranium metal

with the stoichiometric ratio for  $UI_3$  is reasonable. Although acceptable curve resolutions could be performed only down to 0.4 L  $I_2$  exposure, where the  $UI_3/U$  metal ratio  $\approx 0.05$ , the fact that the  $I/U$  absolute atomic ratio changes in a linear fashion as a function of  $I_2$  exposure (see Fig. 17), leads us to suggest that  $UI_3$  is formed also at lower coverages.

#### 3.4.2 $UI_3$ Surface Layer Thickness

It is significant to note that the U(OPV) Auger spectra recorded at 2.9 L and at 60.3 L are nearly identical. By comparison, the XPS spectra measured at the same exposures are not superimposable. We suggest that such differences arise from the different mean free paths of the electrons being analyzed. The Auger spectra are recorded for electrons whose kinetic energy is of the order of 100 eV, while the kinetic energy of the U 4f electrons measured in the XPS spectra is about 875 eV. From the reported (24,65) variation of electron mean free path,  $\lambda$ , with kinetic energy we take  $\lambda = 4 \text{ \AA}$  and  $\lambda = 12 \text{ \AA}$  for 100 eV and 875 eV electrons in U metal, respectively. Regarding the increase for  $\lambda$  in compounds, as discussed below, we estimate for the  $UI_3$  overlayer  $\lambda(100 \text{ eV}) \approx 8 \text{ \AA}$  and  $\lambda(875 \text{ eV}) \approx 24 \text{ \AA}$ , respectively. We recognize that the actual sampling depth is approximately three times the mean free path (95 % of the electrons occur from the depth range 0 to  $3\lambda$ ) (28a,48). Taking the escape depth characteristics into account, from the AES results we suggest that completion of a  $UI_3$  layer of about 24  $\text{\AA}$  occurs following a 2.9 L  $I_2$  exposure. For the XPS measurements we observe that the U 4f spectra are void (<5 %) of uranium metal contributions after an exposure of 40 L  $I_2$ . From this we conclude that a  $UI_3$  layer measuring approximately 72  $\text{\AA}$  is completed at 40 L  $I_2$  exposure.

The differences in the depth of  $UI_3$  layer formation, as indicated by the AES and XPS spectra, are also reflected in the adsorption profile (Fig. 17). It is noted in the range of 1.5 to 2 L  $I_2$  exposure that both XPS and AES curves begin to deviate from linearity. Further the observation of only little change in the AES spectra (120-60 eV) suggests that above 2 to 3 L  $I_2$  exposure the formation of a  $UI_3$  layer is complete. The beginning of the non-linear portion in the adsorption profile would thus correspond to the start of  $UI_3$  sub-surface generation which continues to saturation.

It is of interest to evaluate more precisely the  $UI_3$  layer thickness after an exposure (2.9 L  $I_2$ ) which we believe corresponds to the completion of a uniform

overlayer of  $UI_3$  on uranium. We use the XPS data obtained at a 2.9 L  $I_2$  exposure. The thickness is calculated using the expression presented by Carlson and McGuire (66) and cast in angular dependent form by others (67,68):

$$d = \lambda_o \cos \phi \left[ \ln \left( 1 + \frac{\lambda_m n_m}{\lambda_o n_o} r \right) \right] \quad (5)$$

where the terms are

- d = surface overlayer thickness
- $\phi$  = the electron take-off angle, relative to the surface normal;  $10^\circ$
- $n_m$  = concentration of metal atoms in substrate; U density 19.05 g/cm<sup>3</sup> (69)
- $n_o$  = concentration of metal atoms in overlayer compound; U atom density 2.61 g/cm<sup>3</sup> ( $UI_3$  density 6.78 g/cm<sup>3</sup> (64))
- $\lambda_m$  = mean free path for electrons in metal substrate; 12 Å for U 4f<sub>7/2</sub> electrons in U metal (24,65)
- $\lambda_o$  = mean free path for electrons in overlayer compound; 24 Å for U 4f<sub>7/2</sub> electrons in  $UI_3$  (estimated, see text)
- r = ratio of  $UI_3$  overlayer and U metal U 4f<sub>7/2</sub> photopeak intensities, taken from curve resolved spectra.

For this calculation we estimate the mean free path for U 4f<sub>7/2</sub> electrons in  $UI_3$  to be 24 Å or twice the value for the uranium metal electrons. Others have shown (65,68) that the electron mean free path for metal oxides is of the order of 1.5 to 3.0 times the value for the metal. We make a conservative estimate that for  $UI_3$  the value is two times the metal value. Following this we calculate the surface  $UI_3$  thickness to be 39 Å. If 36 Å is estimated for the  $UI_3$  electron mean free path (i.e.  $3 \lambda_m$ ), the calculated surface thickness is 48 Å. These calculations yield an order of magnitude thickness for the  $UI_3$  overlayer in these studies with polycrystalline uranium and should reasonably be accurate to within  $\pm 50$  %. In the absence of studies using single crystals and LEED or other surface structural results we are not able to make any suggestions regarding crystal reorganizational processes that occur upon formation of the  $UI_3$  overlayer.

### 3.4.3 Kinetics

The kinetics of adsorption can be discussed by considering the results presented in the adsorption profile (Fig. 17). The experimental fractional coverage results,  $\theta = 1$  at saturation, can be evaluated from Fig. 17 by knowing that the I/U ratios

at saturation are 3.0 and 2.1 for XPS and AES measurements, respectively. A linear increase in the I/U ratios is found up to an exposure of about 1.5 to 2.0 L I<sub>2</sub> which corresponds to  $\theta = 0.5$ . Such a linear dependence is indicative of a constant sticking probability and that the kinetics of adsorption probably follow a precursor state model (51,52,54,55,58,59). In such a precursor state physisorbed iodine would likely correspond to the initial state. In attempting to fit our results to a kinetic model it can readily be shown that the data behavior shown in Fig. 17 does not fit a second-order model (51,54) as might be expected for a dissociative adsorption process. If we use the simple first-order Langmuir model (51,54), we see in Fig. 20 that the data points exhibit a linear dependence up to an exposure of 3-4 L I<sub>2</sub>. The linearity of the fit over a wider exposure range is not improved significantly using the model proposed by Kisliuk (52). The reasonably linear fit in the exposure range 0 to 4 L I<sub>2</sub> indicates that the sticking probability is proportional to the fraction of unoccupied surface sites. The change in the slope of the curve in Fig. 20 is observed for both XPS and AES results. We commented above that the uranium (OPV) AES and 4f XPS results suggested the completion of a uranium iodide layer at an exposure of about 3 L I<sub>2</sub>. It is probable that the change in slope is related to the completion of the uranium iodide overlayer and that the lower slope at higher exposures may be characteristic of the reaction of iodine with a UI<sub>3</sub> overlayer on uranium metal. In this regard it seems reasonable that the I<sub>2</sub> sticking probability on a UI<sub>3</sub> surface would not be equal to that on a clean uranium surface. Further it is likely that the rate of I<sub>2</sub> reaction with uranium covered by a uranium-iodide overlayer would be slower than for the clean metal. The rate would also depend on the rate of iodine migration to sublayer uranium or, alternatively, uranium transport from the bulk to the UI<sub>3</sub> overlayer.

In other investigations of the adsorption of I<sub>2</sub> on metals a dissociative adsorption process is presumed (55,59), but no spectroscopic evidence for chemical changes at the metal surface, especially electron transfer from the metal to iodine, was presented. However, an interpretation of XPS binding energies among other spectral characteristics led to the suggestion that iodine (I<sub>2</sub>) adsorbed on Ag(111) yields an iodine species dissimilar to iodide in AgI (36). In the present study it is found that significant electron transfer accompanies I<sub>2</sub> adsorption. Our interpretation of the individual features of the AES and XPS spectra, particularly with regard to the surface composition obtained from the analysis of electrons of different kinetic energies, suggests the initial formation of a uranium iodide (UI<sub>3</sub>) overlayer. The formation of a thick stoichiometric UI<sub>3</sub> layer proceeds after the overlayer is complete, and the rate of completion of the sublayer is slower than for the overlayer.

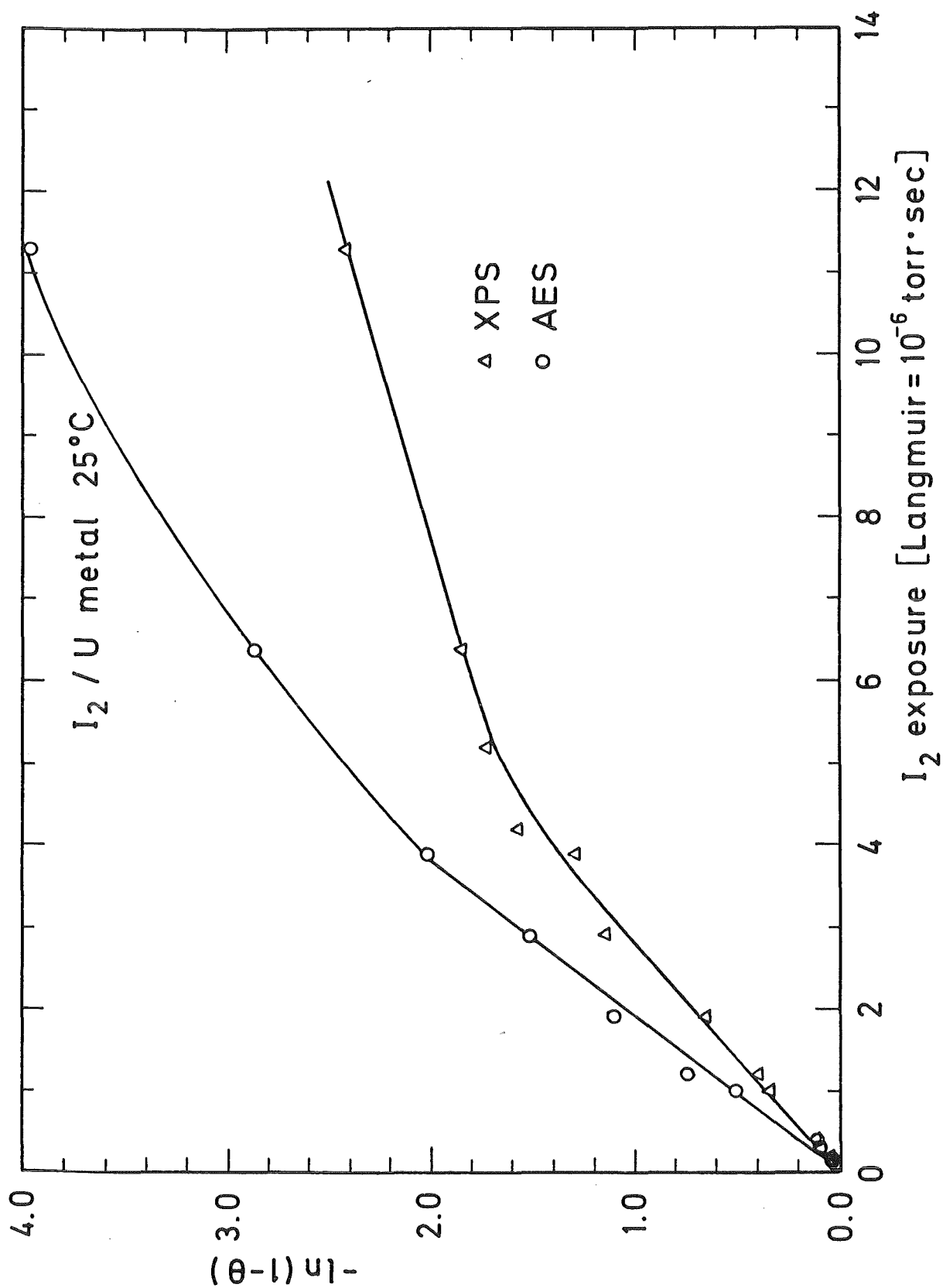


Fig. 20: Integrated rate expression for a first-order Langmuir model of adsorption  $f(\theta) = (-\ln(1-\theta) \propto \text{exposure})$  applied to the data of fig. 17 (adsorption of iodine on uranium metal)

### 3.5 Adsorption of Molecular Iodine on Uranium Dioxide

The adsorption of molecular iodine on uranium dioxide was investigated at 25 °C for I<sub>2</sub> exposures in the range 0.05 to 75 L I<sub>2</sub>. The XPS binding energy results for U 4f<sub>7/2</sub>, I 3d<sub>5/2</sub>, O 1s and the kinetic energy data for the I(M<sub>4</sub>N<sub>4,5</sub>N<sub>4,5</sub>) and U(OPV) transitions are collected in Table 3. The U 4f XPS spectra exhibit no changes in peak shape or binding energy after adsorption of I<sub>2</sub> up to saturation. Uranium AES spectra in the kinetic energy range 130-50 eV for selected I<sub>2</sub> exposures are shown in Fig. 21. The spectra also exhibit no changes in shape or in the kinetic energy of the transitions. These observations show that significant chemical changes for uranium are absent. The difficulties of studying iodine adsorption on oxide surfaces via Auger processes is demonstrated in Fig. 21. In Fig. 21 we show derivative curves, measured using an analyzer retard ratio = 4, in the O(KLL) and I(MNN) energy regions for clean UO<sub>2</sub> and after the adsorption of 0.3, 1.0 and 29.0 L I<sub>2</sub>. Although evidence for the adsorption of I<sub>2</sub> is apparent, evaluation of the changes in the I(MNN) peak intensity with exposure is difficult. For this reason the quantitative aspects of I<sub>2</sub> adsorption on UO<sub>2</sub> have been obtained using XPS results. The adsorption profile expressed as the I/U atomic (XPS) or intensity ratio (AES) vs. I<sub>2</sub> exposure is presented in Fig. 22. We include the measured I/U AES intensity ratio as a function of exposure so as to be complete in our presentation of the results. The I/U XPS atomic ratio at saturation is 0.53. This value is 5.7 times lower than the ratio for I<sub>2</sub> adsorbed on uranium metal.

#### 3.5.1 Interpretation of XPS Binding Energies

The iodine 3d<sub>5/2</sub> electron binding energies at low I<sub>2</sub> exposures on UO<sub>2</sub> are lower than the value reported by others (38,39) for I<sub>2</sub> (solid) but equal (within experimental error) to the value given by Sherwood (42) and to the result in this study (Table 3). At higher I<sub>2</sub> exposures the I 3d<sub>5/2</sub> binding energy occurs at 619.5 ± 0.1 eV which is ≈0.4 eV lower than our value for I<sub>2(s)</sub>. This small shift could indicate a dissociative adsorption of I<sub>2</sub> to yield a U-O-I type surface species. If we consider the U-O-I surface bond, it is probable that electron transfer to electronegative oxygen would occur, and this would have the effect of reducing electron density at iodine. Formally this process would yield a hypoiodite surface species whose binding energy would be expected to be greater than that for I<sub>2(s)</sub> (42) or iodine as iodide. We observe a lower binding energy for adsorbed iodine, and we do not detect any iodine species at binding energies

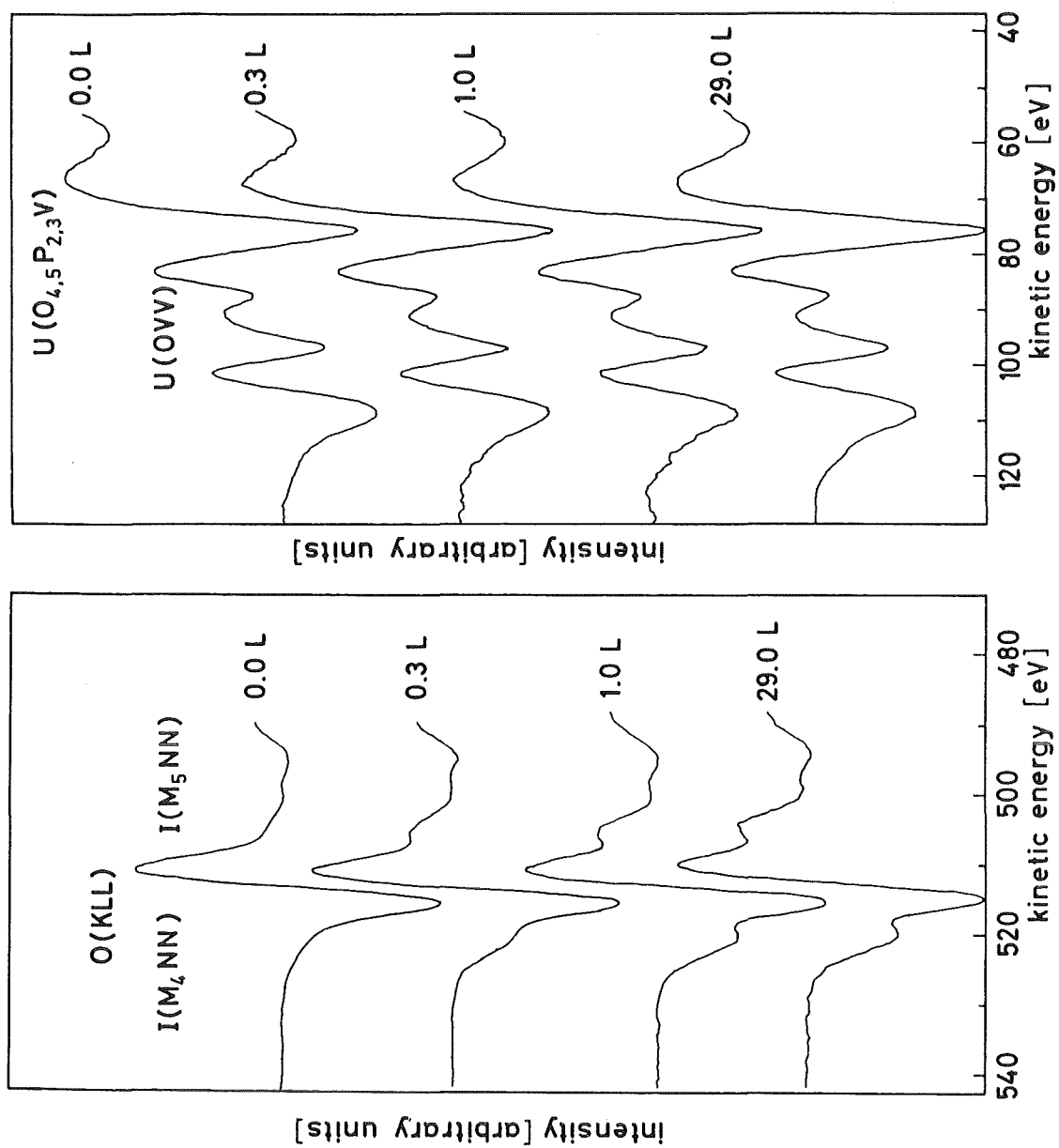


Fig. 21: Auger spectra of the I(MNN)-O(KLL) and U(OPV)-U(OVV) energy regions as a function of I<sub>2</sub> exposure (1 L = 10<sup>-6</sup> torr · sec) on uranium dioxide

greater than that for  $I_{2(s)}$ . The binding energy results are thus inconsistent with the formation of a U-O-I bond via a dissociative process.

An additional dissociative process could involve the formation of an iodine-uranium bond with reduction of iodine and oxidation of uranium(IV) to uranium(V) as shown:



In the XPS and AES spectra following  $I_2$  adsorption we observe no alterations attributable to uranium oxidation. However, we recognize that the magnitude of such shifts could be small. Thibaut et al. (37) have measured the U 4f<sub>7/2</sub> BE of  $UO_2Br$  as 380.3 eV. We can estimate from the data presented (37) that the binding energy shift for a  $UO_2I$  type species would be not greater than 0.5 eV compared to the U 4f<sub>7/2</sub> BE of  $UO_2Br$ . Evidence for U(V) species with shifts not greater than 0.5 eV would be difficult to extract from XPS spectra. Although shifts larger than 0.5 eV in the U(OPV) kinetic energy could be expected due to final state effects (29) (see Table 3), our AES results do not reflect any change in uranium chemistry.

Non-dissociative adsorption of  $I_2$  on the oxide surface, where electron repulsive effects between iodine and oxygen could arise, might lead to a lowering of the iodine electron binding energy as a result of the repulsion. As noted in Table 3, we find a slightly lower electron binding energy for adsorbed iodine at high  $I_2$  exposures compared to solid iodine. The X-ray induced Auger results are more useful in identifying adsorbed molecular  $I_2$ . Conceptually we imagine that an  $I_2$  adsorbate on a solid  $I_2$  substrate corresponds to  $I_{2(s)}$  while  $I_2$  adsorbed on  $UO_2$  corresponds to an  $I_2$  admolecule on an electronegative oxide surface. As a consequence of this we suggest that the principal differences in the measured kinetic energies arise from extra-atomic relaxation effects. In the case of solid  $I_2$  other iodine molecules relax the final ion state while for  $I_2$  on  $UO_2$  surface oxide ions are polarized to relax the hole. The iodine Auger electron kinetic energy and the Auger parameter,  $\alpha$ , for  $I_2$  adsorbed on  $UO_2$  are  $\approx 2$  eV lower than that for  $I_{2(s)}$ . The magnitude and the sign of the difference in electron kinetic energy suggest that in the final ion state greater electron polarizability occurs in the case of  $I_{2(s)}$ . The polarization of neighboring iodine molecules screens the final state making it more repulsive, thus resulting in a greater kinetic energy for the ejected Auger electron. By comparison the polarizability of oxygen on the uranium dioxide surface is not as great and the screening effect is expected to be smaller. A smaller screening effect would result in a lower kinetic energy

for the iodine Auger transition which is what we observe experimentally. On the other hand an effective screening process could be electron transfer to the core hole by uranium 5f electrons. We can comment on the direction of the Auger parameter shift in  $I_2/VO_2$  by comparing the screening in  $I_2/U$ . For  $I_2/U$  compared to  $I_{2(s)}$  we find a higher (0.2 to 0.3 eV) Auger parameter,  $\alpha$ , at low  $I_2$  exposures which we attribute to U 5f electron screening. For  $VO_2$  the U 5f electrons are bound more tightly than the U 5f electrons in uranium metal,  $\Delta E (5f_{VO_2} - 5f_U) = 1.1$  eV. Also the U 5f electron band overlaps with the uranium-oxygen band at about 6 eV so that the availability of the 5f electrons for hole neutralization would be less compared to uranium metal. Thus, while the screening by the  $VO_2$  U 5f electrons would be less than that by uranium metal, it is likely that a positive Auger parameter shift would result. It seems reasonable, therefore, that a measured negative Auger parameter shift for  $I_2$  adsorbed on  $VO_2$  results from iodine interaction with less polarizable surface oxide. We suggest that the XPS and AES results can be interpreted to indicate that  $I_2$  adsorption on  $VO_2$  occurs non-dissociatively. The thermal desorption behavior of  $I_2$  adsorbed on  $VO_2$  has been studied in an attempt to gather further evidence for the non-dissociative process.

### 3.5.2 Thermal Desorption

The thermal stability of the  $VO_2:I_2$  adsorbate substrate complex is less than that for the  $U:I_2$  complex. In Fig. 18 we show the change in the XPS I/U atomic ratio following thermal treatment at three different temperatures for a  $VO_2$  surface saturated with  $I_2$ . The ratio decreases in a monotonic manner and at 600 °C it is near zero. In addition we do not detect any changes in uranium or iodine binding energies following heating. It thus appears that heating only desorbs the adsorbate. This finding is in contrast to the observation that the I/U ratio did not change following the heating of  $VO_2$  on which  $CH_3I$  had been adsorbed (see sect. 3.3). In section 3.3 it was argued that dissociative adsorption of  $CH_3I$  occurs on  $VO_2$  with the formation of U-O-I and U-O- $CH_3$  surface species. We have suggested above that non-dissociative adsorption occurs for  $I_2$  on  $VO_2$ . The thermal behavior seems to support this idea indicating that the bonding of  $I_2$  to the surface is weak. That  $I_2$  is not only physisorbed on  $VO_2$  was demonstrated by measuring time dependent spectra at 300 °C and observing no change in the I/U ratio for  $I_2:VO_2$ . These results suggest that the magnitude of the  $I_2-VO_2$  bonding force is certainly greater than the attractive forces in solid  $I_2$  since the temperature for thermal desorption is greater than the sublimation temperature

for I<sub>2</sub> solid. We cannot speculate further on the surface attractive forces, but such attractions would be expected to be weak and to yield small changes in binding energy values as we have already noted.

### 3.5.3 Kinetics

The kinetics of I<sub>2</sub> adsorption were investigated using the data shown in Fig. 22. Because limited data were obtained from the AES measurements, only the XPS results were used in the analysis. In the adsorption profile we observe a linear increase in the I/U ratio as a function of exposure up to a fractional coverage of  $\theta = 0.6$ . This coverage corresponds to I/U = 0.33 at 0.4 L I<sub>2</sub> exposure. In Fig. 23 we show the treatment of the adsorption kinetic behavior modelled as a first-order ( $-\ln(1-\theta)$ ) and as a second-order ( $\frac{\theta}{1-\theta}$ ) process. The  $f(\theta) = (\frac{\theta}{1-\theta})$  vs I<sub>2</sub> exposure treatment exhibits linear behavior up to an exposure of 4 L I<sub>2</sub> which corresponds to  $\theta = 0.93$ . The simplest interpretation of this result is that either a dissociative adsorption process occurs or that two adsorption sites are required for each adsorbate molecule. Based on our previous discussion, where we indicated that the dissociation of I<sub>2</sub> appears unlikely, we favor the latter interpretation. Acceptance of the non-dissociative process would lead us to conclude that oxygen atoms are the principal surface sites for adsorption, since we have tried to show that the thermal and spectral characteristics are inconsistent with the formation of U-I bonds. We are not able to study surface structural changes that accompany adsorption. During these experiments we were not able to determine the chemical nature of desorbed iodine. We summarize the discussion by affirming that I<sub>2</sub> is adsorbed non-dissociatively on UO<sub>2</sub> and that the surface spectroscopic results and thermal desorption findings are consistent with this conclusion.

## 4. SUMMARY

We have examined the adsorption of CH<sub>3</sub>I and of molecular iodine on clean uranium metal and on stoichiometric UO<sub>2</sub> surfaces at 25 °C. In case of CH<sub>3</sub>I adsorption both substrates lead to dissociative surface chemical reactions. For the uranium metal substrate the species formed could be identified to be UC and UI<sub>3</sub>. For CH<sub>3</sub>I adsorption on UO<sub>2</sub>, however, a unique assignment of the surface reaction products was not possible.

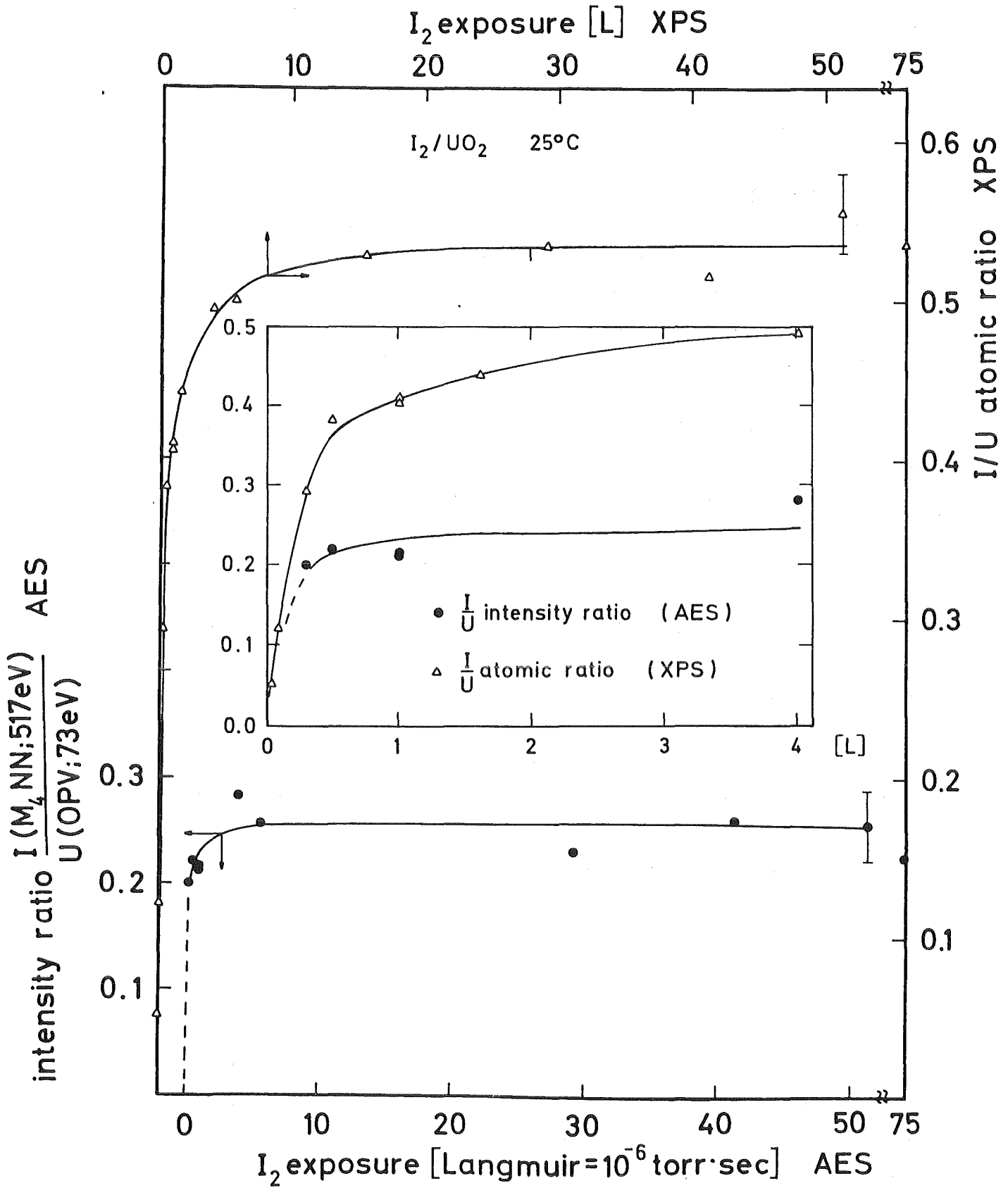


Fig. 22: AES intensity ratio and XPS atomic ratio vs. I<sub>2</sub> exposure on uranium dioxide. The inset shows an expansion of the low exposure region

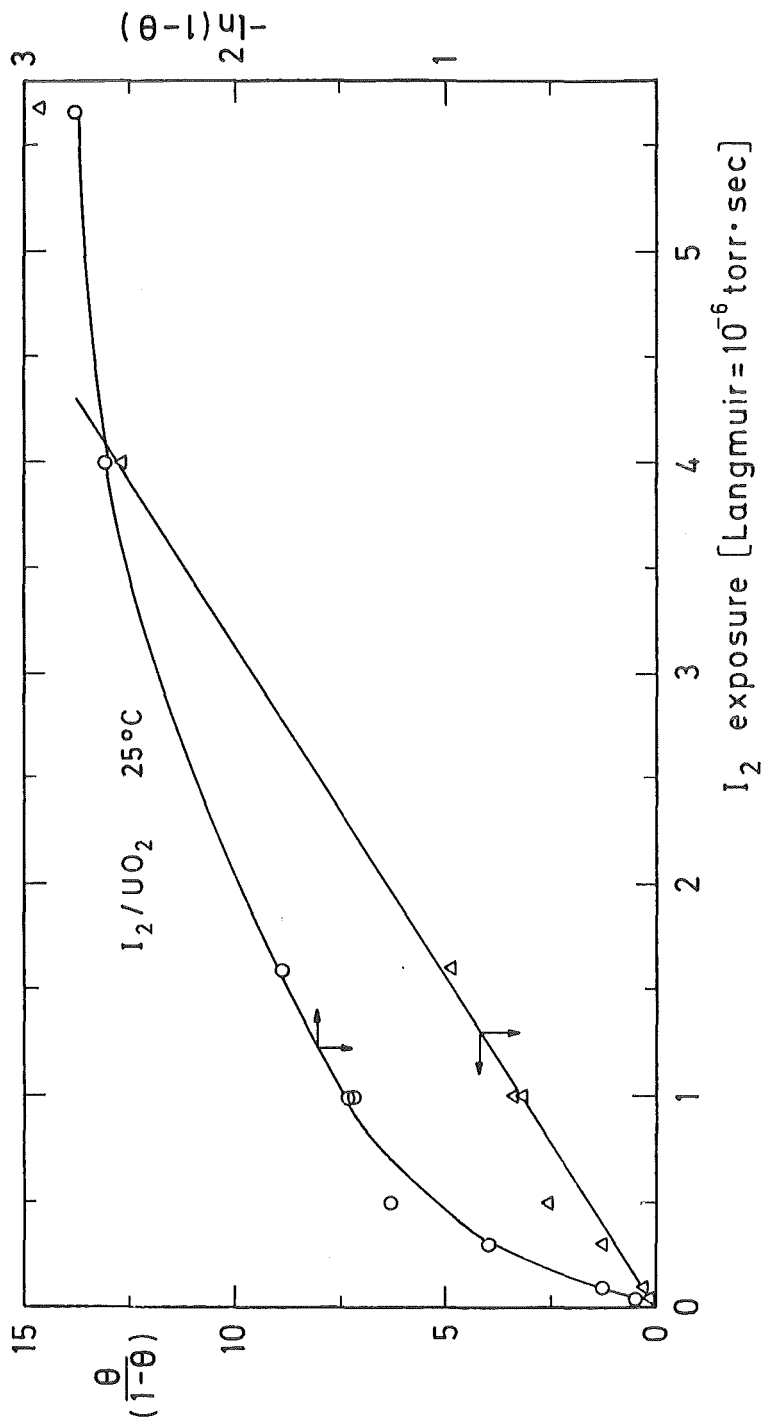


Fig. 23: Integrated rate expressions for Langmuir first-order  $f(\theta) = (-\ln(1-\theta) \propto \text{exposure})$  and second-order  $f(\theta) = \left(\frac{\theta}{1-\theta} \propto \text{exposure}\right)$  models of adsorption applied to the XPS data of fig. 22 (adsorption of iodine on uranium dioxide)

In adsorption of  $I_2$  on U metal the measured kinetic and binding energies of Auger and photoelectrons as well as the I/U intensity ratios clearly indicated a dissociative process with formation of  $UI_3$ . After exposure to 40 L  $I_2$ , approximately corresponding to saturation, we deduced a thickness of the  $UI_3$  layer of  $\approx 70 \text{ \AA}$ .

The study of  $I_2$  exposure to  $UO_2$  revealed no indication of a dissociative adsorption. In contrast to  $CH_3I$  adsorption on  $UO_2$ , where the I/U intensity ratio remained constant with increasing temperature, we observed for  $I_2$  on  $UO_2$  a monotonic decrease of the I/U ratio with increasing temperature indicating normal thermal desorption of non-dissociatively adsorbed  $I_2$ .

A study of the kinetic behavior of the adsorption processes under investigation showed that  $CH_3I$  adsorption on U metal could be fit to a precursor kinetic model. Among others this finding led to the suggestion that adsorption of  $CH_3I$  via a U-I bond occurs as the rate controlling process.

In contrast the data for  $I_2$  adsorption on U metal could be fitted to a first order kinetic model only up to an exposure of  $\approx 3 \text{ L}$  which corresponds to completion of a  $UI_3$  overlayer. Deviations from this kinetic behavior for greater exposures are probably due to a change in the rate of the reaction of  $I_2$  with a U metal surface and a  $UI_3$  covered U surface, respectively.

Finally, a comparison of the different adsorbate/substrate atomic ratios at saturation coverage shall be performed. For  $CH_3I$  adsorption on U metal at  $\approx 2 \text{ L}$   $I/U = 0.3$  and  $C/U = 0.09$  were found, while for  $\approx 5 \text{ L}$   $CH_3I$  on  $UO_2$  the ratios were  $I/U = 0.034$  and  $C/U = 0.03$ . These ratios indicate a loss of carbon in the reaction with U metal ( $I/C \approx 3$ ) in contrast to the reaction with  $UO_2$  ( $I/C \approx 1$ ). The I/U ratios show that the quantity of primarily adsorbed  $CH_3I$  is  $\approx 10$  times larger for U metal than for  $UO_2$ . For  $I_2$  adsorption the atomic ratios at saturation were found to be  $I/U = 3.04$  for 40 L  $I_2$  on U metal (corresponding to formation of a thick  $UI_3$  layer) and  $I/U = 0.53$  for 10-15 L  $I_2$  on  $UO_2$ . One recognizes that also in this case the quantity of the adsorbate (adsorbed  $I_2$ ) is much larger for U metal than for  $UO_2$ , probably due to the lower reactivity of oxide surfaces.

### Acknowledgements

The authors thank Dr. C. Politis, Institut für Angewandte Kernphysik I, Kernforschungszentrum Karlsruhe, for the preparation of the UC sample. One of us (J.G.D.) thanks the Department of Chemistry and Virginia Tech for granting an educational leave during which time this work was carried out and expresses appreciation to Kernforschungszentrum Karlsruhe for making the leave enjoyable and productive.

## REFERENCES

1. W.P. Ellis, *Surface Sci.*, 61 (1976) 37
2. W.P. Ellis and B.D. Campbell, *J. Appl. Phys.*, 41 (1970) 1858
3. P.R. Norton, R.L. Tapping, D.K. Creber and W.J.L. Buyers, *Phys. Rev. B* 21 (1980) 2572
4. B.W. Veal and D.J. Lam, *Phys. Rev. B* 10 (1974) 4902
5. J.C. Fuggle, A.F. Burr, L.M. Watson, D.J. Fabian and W. Lang, *J. Phys. F* 4 (1974) 335
6. G.C. Allen, J.A. Crofts, M.T. Curtis, P.M. Tucker, D. Chadwick and P.J. Hampson, *J. Chem. Soc., Dalton* (1974) 1296
7. S.B. Nornes and R.G. Meisenheimer, *Surface Sci.*, 88 (1979) 191
8. W.P. Ellis, *Surface Sci.*, 109 (1981) L567
9. N. Beatham, A.F. Orchard and G. Thornton, *J. Electron Spectrosc. Relat. Phenom.*, 19 (1980) 205
10. G.C. Allen and P.M. Tucker, *J. Chem. Soc., Dalton* (1973) 470
11. A.W. Castleman, I.N. Tang and H.R. Munkelwitz, *J. Inorg. Nucl. Chem.*, 30 (1968) 5
12. "Control of Iodine in the Nuclear Industry", Technical Reports Series No. 148, International Atomic Energy Agency, Vienna, 1973
13. M. Nakashima and E. Tachikawa, *J. Nucl. Sci. Tech.*, 15 (1978) 849
14. G.C. Allen, P.M. Tucker and J.W. Tyler, *J. Chem. Soc. Chem. Comm.* (1981) 691
15. Y.A. Teterin, V.M. Kulakov, A.S. Baev, N.B. Nevzorov, I.V. Melnikov, V.A. Streltsov, L.G. Mashirov, D.N. Suglobov and A.G. Zelenkov, *Phys. Chem. Minerals*, 7 (1981) 151
16. L.E. Cox, *J. Electron Spectrosc. Relat. Phenom.*, 26 (1982) 167
17. S. Evans, *J. Chem. Soc., Faraday Trans. II*, 73 (1977) 1341
18. G.C. Allen and R.K. Wild, *J. Chem. Soc., Dalton* (1974) 493
19. R. Bastasz and T.E. Felter, *Phys. Rev. B* 26 (1982) 3529
20. J.J. Katz and G.T. Seaborg, The Chemistry of Actinide Elements, Methuen, London, 1957, p. 148
21. F.A. Cotton and G. Wilkinson, Advanced Inorganic Chemistry, Interscience, New York, 4th Ed., 1980, p. 1028-1042
22. E.H.P. Cordfunke, The Chemistry of Uranium, Elsevier Publishing Co., Amsterdam, 1969, p. 138-164
23. L.D. Roberts, D.E. Lavalley and R.A. Erickson, *J. Chem. Phys.*, 22 (1954) 1145

24. T.A. Carlson, Photoelectron and Auger Spectroscopy, Plenum Press, New York, 1975
25. D.A. Shirley, Phys. Rev. B5 (1972) 4709
26. J.H. Scofield, J. Electron Spectrosc. Relat. Phenom., 8 (1976) 129
27. J.C. Fuggle and N. Martensson, J. Electron Spectrosc. Relat. Phenom., 21 (1980) 275
28. C.D. Wagner, "The Role of Auger Lines in Photoelectron Spectroscopy" in Handbook of X-ray and Ultraviolet Photoelectron Spectroscopy, ed. D. Briggs, Heyden, London, 1977, p. 249-272
- 28a. D. Briggs, "XPS as an Analytical Technique", *ibid.* p. 153-181
29. C.D. Wagner, L.H. Gale and R.H. Rymond, Anal. Chem., 51 (1979) 466
30. C.D. Wagner, Discussion Faraday Soc., 60 (1975) 291
31. A.A. Bakke, H.-W. Chen and W.L. Jolly, J. Electron Spectrosc. Relat. Phenom., 20 (1980) 333
32. L. Ramqvist, J. Appl. Phys., 42 (1971) 2113
33. M.A. Chesters, B.J. Hopkins, A.R. Jones and R. Nathan, Surface Sci., 45 (1974) 740
34. R. Mason and M. Textor, Proc. Roy. Soc. London A, 356 (1977) 47
- 35a. J.G. Dillard, H. Moers, H. Klewe-Nebenius, G. Kirch, G. Pfennig and H.J. Ache, Conference Abstracts, SCADEG-AMSEL Meeting, De Eemhof, The Netherlands, May 3-6, 1983 (to be published in Spectrochimica Acta B)
- 35b. J.G. Dillard, H. Moers, H. Klewe-Nebenius, G. Kirch, G. Pfennig and H.J. Ache (submitted to J. Phys. Chem.)
36. G.K. Wertheim, S.B. DiCenzo and D.N.E. Buchanan, Phys. Rev. B 25 (1982) 3020
37. E. Thibaut, J.-P. Boutique, J.J. Verbist, J.-C. Levet and H. Noel, J. Am. Chem. Soc., 104 (1982) 5266
38. W.R. Salaneck, H.R. Thomas, R.W. Bigelow, C.B. Duke, E.W. Plummer, A.J. Heeger and A.G. MacDiarmid, J. Chem. Phys., 72 (1980) 3674
39. W.R. Salaneck, R.W. Bigelow, H.-J. Freund and E.W. Plummer, Phys. Rev. B 24 (1981) 2403
40. S.B. DiCenzo, G.K. Wertheim and D.N.E. Buchanan, Phys. Rev. B 24 (1981) 6143
41. S.B. DiCenzo, G.K. Wertheim and D.N.E. Buchanan, Surface Sci., 121 (1982) 411
42. P.M.A. Sherwood, J. Chem. Soc., Faraday Trans. II, 72 (1976) 1805
43. M.G. Mason, Phys. Rev. B 11 (1975) 5094
44. S.W. Gaarenstroom and N. Winograd, J. Chem. Phys., 67 (1977) 3500

45. S.P. Kowalczyk, R.A. Pollak, F.R. McFeely, L. Ley and D.A. Shirley, Phys. Rev. B 8 (1973) 2387
46. J.T. Yates and N.E. Erickson, Surface Sci., 44 (1974) 489
47. T.E. Madey, J.T. Yates and N.E. Erickson, Chem. Phys. Lett., 19 (1973) 487
48. M.W. Roberts, "Photoelectron Spectroscopy and Surface Chemistry" in Advances in Catalysis, Vol. 29, eds. D.D. Eley, H. Pines and P.B. Weisz, Academic Press, 1980, p. 55
49. P.A. Dowben and R.G. Jones, Surface Sci., 89 (1979) 114
50. J.G. Dillard, H. Moers, H. Klewe-Nebenius and H.J. Ache, Fall 1982, Kernforschungszentrum Karlsruhe (unpublished results)
51. W.H. Weinberg, C.M. Comrie and R.M. Lambert, J. Catal., 41 (1976) 489
52. P. Kisliuk, J. Chem. Phys. Solids, 3 (1957) 95; 5 (1958) 78
53. C. Kohrt and R. Gomer, J. Chem. Phys., 52 (1970) 3283
54. J.C. Fuggle, T.E. Madey, M. Steinkilberg and D. Menzel, Surface Sci., 52 (1975) 521
55. P.A. Dowben and R.G. Jones, Surface Sci., 88 (1979) 348 (and reference therein)
56. S.A. Cochran and H.H. Farrell, Surface Sci., 95 (1980) 359
57. P.A. Dowben and R.G. Jones, Surface Sci., 84 (1979) 449
58. R.G. Jones and D.L. Perry, Surface Sci., 88 (1979) 331
59. K.J. Rawlings, G.G. Price, and B.J. Hopkins, Surface Sci., 95 (1980) 245
60. D.K. Craig, Health Phys., 12 (1966) 1047
61. D.O. Campell, A.P. Malinauskas, and W.R. Stratton, Nuclear Technol., 53 (1981) 111
62. S.H. Shann and D.R. Olander, J. Nucl. Materials, 113 (1983) 234
63. S.P. Kowalczyk, L. Ley, F.R. McFeely, R.A. Pollak, and D.A. Shirley, Phys. Rev. B, 9 (1974) 381
64. J.H. Levy, J.C. Taylor, and P.W. Wilson, Acta Cryst. B, 31 (1975) 880
65. C.R. Brundle, J. Vac. Sci. Technol., 11 (1974) 212.
66. T.A. Carlson and G.E. McGuire, J. Electron Spectrosc. Relat. Phenom., 1 (1972/73) 161
67. A.F. Carley and M.W. Roberts, Proc. Roy. Soc., London, A 363 (1978) 403
68. A. Shephard, R.H. Hewitt, W.E. Baittinger, G.J. Slusser, N. Winograd, G.L. Ott, and W.N. Delgass "XPS and SIMS: A multitechnique approach to surface analysis", Quantative Surface Analysis of Materials, ASTM STP 643, N.S. McIntyre, ed., ASTM, 1978, p. 187-203
69. CRC Handbook of Chemistry and Physics, 62nd Ed., R.C. Weast and M.J. Astle, eds., CRC Press, Boca Raton, FL, 1981